



ELSEVIER

Applied Numerical Mathematics 43 (2002) 9–44



APPLIED
NUMERICAL
MATHEMATICS

www.elsevier.com/locate/apnum

Krylov subspace techniques for reduced-order modeling of large-scale dynamical systems

Zhaojun Bai

Department of Computer Science, University of California, Davis, CA 95616, USA

Abstract

In recent years, a great deal of attention has been devoted to Krylov subspace techniques for reduced-order modeling of large-scale dynamical systems. The surge of interest was triggered by the pressing need for efficient numerical techniques for simulations of extremely large-scale dynamical systems arising from circuit simulation, structural dynamics, and microelectromechanical systems. In this paper, we begin with a tutorial of a Lanczos process based Krylov subspace technique for reduced-order modeling of linear dynamical systems, and then give an overview of the recent progress in other Krylov subspace techniques for a variety of dynamical systems, including second-order and nonlinear systems. Case studies arising from circuit simulation, structural dynamics and microelectromechanical systems are presented.

© 2002 IMACS. Published by Elsevier Science B.V. All rights reserved.

Keywords: Dynamical systems; Reduced-order modeling; Transfer function; Stability; Passivity; Moment-matching; Padé approximation; Krylov subspace technique

1. Introduction

The continual and pressing need for accurately and efficiently simulating dynamical behaviors of complex physical systems arising from computational science and engineering has led to increasingly large and complex models. Reduced-order modeling techniques play an indispensable role by providing an efficient computational prototyping tool to replace such a large-scale model by an approximate smaller model, which is capable of capturing dynamical behavior and preserving essential properties of the larger one.

A myriad of reduced-order modeling methods has been presented in various fields. Most of these methods fall into two categories. The first one is comprised of the techniques based on the optimization of the reduced-order model according to a suitably chosen criterion. The second category consists of the

E-mail address: bai@cs.ucdavis.edu (Z. Bai).

methods which preserve exactly a limited number of parameters of the original model. The work of [25] provides a survey of early work on these methods. Over the past several years, Krylov subspace based techniques have emerged as one of the most powerful tools for reduced-order modeling of large-scale systems. We would like to call the reader's attention to recent surveys on the topic [27,29,3], which are complimentary to this work.

In order to introduce first-time readers to this topic, we will begin with a tutorial of Krylov subspace techniques for reduced-order modeling of linear dynamical systems, specifically, on moment-matching methods based on the Lanczos process. Then we give an overview of the recent progress of other methods for linear systems. We will also discuss the work which extends the Krylov subspace techniques for reduced-order modeling of second-order, semi-second-order, and nonlinear systems. There are plenty of questions remaining unsolved with regard to those methods discussed in this paper, particularly on semi-second-order systems and nonlinear systems. We will list these open questions throughout the paper.

Our motivation for studying reduced-order modeling techniques stems from the need for efficient simulation tools for dynamical systems arising in circuit simulation, structural dynamics and micro-electromechanical systems (MEMS). We will report our experiences with case studies arising from these applications.

To encourage first-time readers to try out some of approaches discussed in this paper, we have set up a web site at <http://www.cs.ucdavis.edu/~bai> to include basic implementation of some methods, along with some test data. We hope this will also be regarded as an effort to exchange software and test problems amongst researchers and practitioners who are interested in using these tools.

The rest of this paper is organized as follows. In Section 2, we introduce linear dynamical systems and associated computational tasks and challenges. Then we give a tutorial on Lanczos process based moment-matching methods for reduced-order modeling of linear systems. The remaining parts of Section 2 are devoted to the discussion of some essential properties associated with linear dynamical systems and how to preserve these properties in a reduced-order model, and finally we review other reduced-order modeling methods for linear systems. In Section 3, we discuss the treatment of second-order systems by the Krylov subspace based methods with the moment-matching property. Sections 4 and 5 report some preliminary work on the generalization of Krylov subspace techniques for semi-second-order and nonlinear systems. Concluding remarks are in Section 6.

With a few exceptions, we follow the notational conventions used in [27,29]. Specifically, we use boldface letters to denote vectors and matrices, $\mathbf{0}$ for zero vectors or matrices, \mathbf{I} for the identity matrix, \mathbf{e}_k for the k th unit vector (the k th column of \mathbf{I}). The dimensions of these matrices and vectors are conformed with dimensions used in the context, \cdot^T denotes transpose, $\mathbf{i} = \sqrt{-1}$, $\Re(s)$ is the real part of a complex variable s and \mathcal{R}, \mathcal{C} denote the sets of real and complex numbers, respectively. We use $\mathcal{R}_{m,n}$ denotes the set of rational functions with real numerator polynomial of degree at most m and real denominator polynomial of degree at most n .

2. Linear dynamical systems

A continuous time-invariant (lumped) multi-input multi-output linear dynamical system is of the form

$$\begin{cases} \mathbf{C}\dot{\mathbf{x}}(t) + \mathbf{G}\mathbf{x}(t) = \mathbf{B}\mathbf{u}(t), \\ \mathbf{y}(t) = \mathbf{L}^T\mathbf{x}(t), \end{cases} \quad (1)$$

with initial condition $\mathbf{x}(0) = \mathbf{x}_0$. Here t is the time variable, $\mathbf{x}(t) \in \mathcal{R}^N$ is a state vector, $\mathbf{u}(t) \in \mathcal{R}^m$ the input excitation vector, and $\mathbf{y}(t) \in \mathcal{R}^p$ the output measurement vector. $\mathbf{C}, \mathbf{G} \in \mathcal{R}^{N \times N}$ are system matrices, $\mathbf{B} \in \mathcal{R}^{N \times m}$ and $\mathbf{L} \in \mathcal{R}^{N \times p}$ are input and output distribution arrays, respectively. N is the state space dimension and m and p are the number of inputs and outputs, respectively. In most practical cases, we can assume that m and p are much smaller than N and $m \geq p$.

Linear systems arise in many applications, such as the network circuit with linear elements [87], structural dynamics analysis with only lumped mass and stiffness elements [22,23], linearization of a nonlinear system around an equilibrium point [27], and a semi-discretization with respect to spatial variables of a time-dependent differential-integral equations [73,88].

The matrices \mathbf{C} and \mathbf{G} in (1) are allowed to be singular, and we only assume that the pencil $\mathbf{G} + s\mathbf{C}$ is *regular*, i.e., the matrix $\mathbf{G} + s\mathbf{C}$ is singular only for a finite number of values $s \in \mathcal{C}$. The assumption that $\mathbf{G} + s\mathbf{C}$ is regular is satisfied for all applications we are concerned with that lead to systems of the form (1). In addition, \mathbf{C} and \mathbf{G} in (1) are general nonsymmetric matrices. However, in some important applications, \mathbf{C} and \mathbf{G} are symmetric, and possibly positive definite or positive semidefinite. For example, with proper formulation, \mathbf{C} and \mathbf{G} are symmetric indefinite for a linear circuit network that consists of only resistors, inductors and capacitors (in short, a linear RLC circuit). An important special case is RC networks consisting of only resistors and capacitors; in this case, one of \mathbf{C} and \mathbf{G} is symmetric positive definite. Note that when \mathbf{C} is singular, the first equation in (1) is a first-order system of linear differential-algebraic equations. The corresponding linear system is called a descriptor system or a singular system.

The linear system of the form (1) is often referred to as the representation of the system in the time domain, or in the state space. Equivalently, one can also represent the system in the frequency domain via a Laplace transform. Recall that for a vector-valued function $\mathbf{f}(t)$, the Laplace transform of $\mathbf{f}(t)$ is defined by

$$\mathbf{F}(s) := \mathcal{L}\{\mathbf{f}(t)\} = \int_0^{\infty} \mathbf{f}(t)e^{-st} dt, \quad s \in \mathcal{C}. \quad (2)$$

The physically meaningful values of the complex variable s are $s = i\omega$, where $\omega \geq 0$ is referred to as the frequency. Taking the Laplace transform of the system (1), we obtain the following frequency domain formulation of the system:

$$\begin{cases} s\mathbf{C}\mathbf{X}(s) + \mathbf{G}\mathbf{X}(s) = \mathbf{B}\mathbf{U}(s), \\ \mathbf{Y}(s) = \mathbf{L}^T\mathbf{X}(s), \end{cases} \quad (3)$$

where $\mathbf{X}(s)$, $\mathbf{Y}(s)$ and $\mathbf{U}(s)$ represents the Laplace transform of $\mathbf{x}(t)$, $\mathbf{y}(t)$ and $\mathbf{u}(t)$, respectively. For simplicity, we assume that we have zero initial conditions $\mathbf{x}(0) = \mathbf{x}_0 = \mathbf{0}$ and $\mathbf{u}(0) = \mathbf{0}$.

Eliminating the variable $\mathbf{X}(s)$ in (3), we see that the input $\mathbf{U}(s)$ and the output $\mathbf{Y}(s)$ in the frequency domain are related by the following $p \times m$ matrix-valued rational function

$$\mathbf{H}(s) = \mathbf{L}^T(\mathbf{G} + s\mathbf{C})^{-1}\mathbf{B}. \quad (4)$$

$\mathbf{H}(s)$ is known as the *transfer function* or *Laplace-domain impulse response* of the linear system (1).

The following types of analysis are typically performed for a given linear dynamical system of the form (1):

- Static (DC) analysis, to find the point to which the system settles in the equilibrium, or rest, condition, namely $\dot{\mathbf{x}}(t) = \mathbf{0}$;

- Steady-state analysis, also called frequency response analysis, to determine the frequency responses $\mathbf{H}(s)$ of the system to external steady-state oscillatory (i.e., sinusoidal) excitation;
- Modal frequency analysis, to find system natural vibrating frequency modes and their corresponding modal shapes;
- Transient analysis, to compute the output behavior $\mathbf{y}(t)$ subject to time-varying excitation $\mathbf{u}(t)$;
- Sensitivity analysis, to determine the proportional changes of the time response $\mathbf{y}(t)$ and/or steady-state response $\mathbf{H}(s)$ to a proportional change in system parameters.

This paper will focus on applying reduced-order modeling techniques for steady-state and transient analysis.

Linear dynamical systems have been studied extensively, especially for the case $\mathbf{C} = \mathbf{I}$, for example, see [49]. Numerous techniques have been developed for performing various analyses of the system. One of the primary computational challenges we are confronted with today is the large state dimension N of the system (1). For example, in circuit simulation and structural dynamics applications, N could be as large as 10^6 . In addition, the differential equations in the system (1) are often stiff from multi-energy and multi-scaling simulation. The system may be required to be analyzed repeatedly for different excitation inputs $\mathbf{u}(t)$.

As a tutorial on Krylov subspace techniques for large-scale linear dynamical systems, in the rest of this section we mostly confine our discussion to single-input single-output systems, i.e., $p = m = 1$. We will use lower case letters \mathbf{b} and \mathbf{l} to denote the input and output distribution vectors, instead of the capital letters \mathbf{B} and \mathbf{L} . Consequently, the transfer function defined in (4) is a scalar function, and will be denoted by $H(s)$. References will be given for the treatments of multi-input multi-output systems.

2.1. Eigensystem methods

Let us first review eigensystem methods as an introduction to the steady-state analysis of the linear system. To compute $H(s)$ about a selected expansion point s_0 , let us set

$$\mathbf{A} = -(\mathbf{G} + s_0\mathbf{C})^{-1}\mathbf{C} \quad \text{and} \quad \mathbf{r} = (\mathbf{G} + s_0\mathbf{C})^{-1}\mathbf{b},$$

where we assume that $\mathbf{G} + s_0\mathbf{C}$ is nonsingular. Then $H(s)$ can be cast as

$$H(s) = \mathbf{l}^T((\mathbf{G} + s_0\mathbf{C}) + (s - s_0)\mathbf{C})^{-1}\mathbf{b} = \mathbf{l}^T(\mathbf{I} - (s - s_0)\mathbf{A})^{-1}\mathbf{r}. \quad (5)$$

In other words, we reduce the representation of the transfer function $H(s)$ using only one matrix \mathbf{A} . Assume that the matrix \mathbf{A} is diagonalizable,

$$\mathbf{A} = \mathbf{S}\mathbf{\Lambda}\mathbf{S}^{-1} = \mathbf{S} \cdot \text{diag}(\lambda_1, \lambda_2, \dots, \lambda_N) \cdot \mathbf{S}^{-1}.$$

Let $\mathbf{f} = \mathbf{S}^T\mathbf{l} = (f_j)$ and $\mathbf{g} = \mathbf{S}^{-1}\mathbf{r} = (g_j)$, then the transfer function $H(s)$ can be expressed as a partial-fraction expansion,

$$H(s) = \mathbf{f}^T(\mathbf{I} - (s - s_0)\mathbf{A})^{-1}\mathbf{g} = \sum_{j=1}^N \frac{f_j g_j}{1 - (s - s_0)\lambda_j} = \rho_\infty + \sum_{\lambda_j \neq 0} \frac{\kappa_j}{s - p_j}. \quad (6)$$

This is known as the *pole-residue representation*. $p_j = s_0 + 1/\lambda_j$ are *poles* of the system,¹ $\kappa_j = -f_j g_j / \lambda_j$ are *residues*, and $\rho_\infty = \sum_{\lambda_j=0} f_j g_j$ is a constant, which corresponds to the poles at infinity (or zero eigenvalues). Note that it costs $\mathcal{O}(N^3)$ operations to diagonalize \mathbf{A} , and only $\mathcal{O}(N)$ operations to evaluate the transfer function $H(s)$ for each given point s .

Unfortunately, in practice, diagonalization of \mathbf{A} is prohibitive when it is ill-conditioned or is too large. As a remedy for the possible ill-conditioning of diagonalization, we may use the numerically stable Schur decomposition. Let $\mathbf{A} = \mathbf{Q}\mathbf{T}\mathbf{Q}^T$ be the Schur decomposition of \mathbf{A} . Then

$$H(s) = \mathbf{l}^T (\mathbf{I} - (s - s_0)\mathbf{A})^{-1} \mathbf{r} = (\mathbf{Q}^T \mathbf{l})^T (\mathbf{I} - (s - s_0)\mathbf{T})^{-1} (\mathbf{Q}^T \mathbf{r}).$$

Now, it costs $\mathcal{O}(N^2)$ to evaluate the transfer function $H(s)$ at each given point s . Alternatively, one can use the Hessenberg decomposition of \mathbf{A} as suggested in [54].

To reduce the cost of diagonalizing \mathbf{A} or computing its Schur decomposition for large N , we may use partial eigendecomposition. This is also referred to as the *modal superposition method*, for example, see [22]. By examining the pole-residue representation (6), it is easy to see that the motivation of this approach comes from the fact that only a few poles (and associated eigenvalues) around the region of frequencies of interest are necessary for the approximation of $H(s)$. Those poles are called the dominant poles. Therefore, to study the steady-state response to an input of the form $\mathbf{u}(t) = \tilde{\mathbf{u}}e^{i\omega t}$, where $\tilde{\mathbf{u}}$ is a constant vector, we express the solution as $\mathbf{x}(t) = \mathbf{S}_k \mathbf{v}(\omega)e^{i\omega t}$, where \mathbf{S}_k contains k selected modal shapes (eigenvectors) of the matrix pair $\{\mathbf{C}, \mathbf{G}\}$ needed to retain all the modes whose resonant frequencies lie within the range of input excitation frequencies. Then one may solve the system

$$(i\omega \mathbf{S}_k^T \mathbf{C} \mathbf{S}_k + \mathbf{S}_k^T \mathbf{G} \mathbf{S}_k) \mathbf{v}(\omega) = \mathbf{S}_k^T \mathbf{B} \tilde{\mathbf{u}} \quad (7)$$

for $\mathbf{v}(\omega)$. Once the selected dominant poles and their corresponding modal shapes \mathbf{S}_k are computed, the problem of computing the steady-state response is reduced to solving the $k \times k$ system (7). In practice, it is typical that only a relatively small number of the modal shapes is necessary, i.e., $k \ll N$. The problem of finding a few modal shapes \mathbf{S}_k within a certain frequency range is one of the well-known algebraic eigenvalue problems in numerical linear algebra [4].

2.2. Reduced-order modeling

The desired attributes of reduced-order modeling of the linear dynamical system (1) include replacing the full-order system by a system of the same type but with a much smaller state-space dimension such that it has an admissible error between the full-order and reduced-order models. Furthermore, the reduced-order model should also preserve essential properties of the full-order system. Such a reduced-order model would let designers efficiently analyze and synthesize the dynamical behavior of the original system within a tight design cycle. Specifically, given the linear dynamical system (1), we want to find a reduced-order linear system of the same form

$$\begin{cases} \mathbf{C}_n \dot{\mathbf{z}}(t) + \mathbf{G}_n \mathbf{z}(t) = \mathbf{B}_n \mathbf{u}(t), \\ \tilde{\mathbf{y}}(t) = \mathbf{L}_n^T \mathbf{z}(t), \end{cases} \quad (8)$$

¹ By a simple exercise, it can be shown that the definition of poles and residues of the system is independent of the choice of the expansion point s_0 .

where $\mathbf{z}(t) \in \mathcal{R}^n$, $\mathbf{C}_n, \mathbf{G}_n \in \mathcal{R}^{n \times n}$, $\mathbf{B}_n \in \mathcal{R}^{n \times m}$, $\mathbf{L}_n \in \mathcal{R}^{n \times p}$, and $\tilde{\mathbf{y}}(t) \in \mathcal{R}^p$. The state-space dimension n of (8) should generally be much smaller than the state-space dimension N of (1), i.e., $n \ll N$. Meanwhile, the output $\tilde{\mathbf{y}}(t)$ of (8) approximates the output $\mathbf{y}(t)$ of (1) in accordance with some criteria for all \mathbf{u} in the class of admissible input functions. Furthermore, the reduced-order system (8) should preserve essential properties of the full-order system (1).

Note that the $p \times m$ matrix-valued transfer function of the reduced-order model (1) is given by

$$\mathbf{H}_n(s) = \mathbf{L}_n^T (\mathbf{G}_n + s\mathbf{C}_n)^{-1} \mathbf{B}_n.$$

Hence, for the steady-state analysis in the frequency domain, the objectives of constructing a reduced-order model (8) include that the reduced-order transfer function $\mathbf{H}_n(s)$ should be an approximation of the transfer function $\mathbf{H}(s)$ of the full-order model over the frequency range of interest with an admissible error, and that $\mathbf{H}_n(s)$ preserves essential properties of $\mathbf{H}(s)$.

2.3. Padé approximation and moment-matching

Note that the scalar transfer function $H(s)$ of (4) is a rational function. More precisely, $H(s) \in \mathcal{R}_{N-1,N}$, where N is the state-space dimension of (1). The Taylor series expansion of $H(s)$ of (5) about s_0 is given by

$$\begin{aligned} H(s) &= \mathbf{I}^T (\mathbf{I} - (s - s_0)\mathbf{A})^{-1} \mathbf{r} = \mathbf{I}^T \mathbf{r} + (\mathbf{I}^T \mathbf{A} \mathbf{r})(s - s_0) + (\mathbf{I}^T \mathbf{A}^2 \mathbf{r})(s - s_0)^2 + \dots \\ &= m_0 + m_1(s - s_0) + m_2(s - s_0)^2 + \dots, \end{aligned} \tag{9}$$

where $m_j = \mathbf{I}^T \mathbf{A}^j \mathbf{r}$ for $j = 0, 1, 2, \dots$, are called *moments* about s_0 . Since our primary concern is large state-space dimension N , we seek to approximate $H(s)$ by a rational function $H_n(s) \in \mathcal{R}_{n-1,n}$ over the range of frequencies of interest, where $n \leq N$. A natural choice of such a rational function is a Padé approximation. A function $H_n(s) \in \mathcal{R}_{n-1,n}$ is said to be an n th Padé approximant of $H(s)$ about the expansion point s_0 if it matches with the moments of $H(s)$ as far as possible. Precisely, it is required that

$$H(s) = H_n(s) + \mathcal{O}((s - s_0)^{2n}). \tag{10}$$

For a thorough treatment of Padé approximants, we refer the reader to [12]. Note that equation (10) presents $2n$ conditions on the $2n$ degrees of freedom that describe any function $H_n(s) \in \mathcal{R}_{n-1,n}$. Specifically, let

$$H_n(s) = \frac{P_{n-1}(s)}{Q_n(s)} = \frac{a_{n-1}s^{n-1} + \dots + a_1s + a_0}{b_n s^n + b_{n-1}s^{n-1} + \dots + b_1s + 1}, \tag{11}$$

where b_0 is chosen to be equal to 1, which eliminates an arbitrary multiplicative factor in the definition of $H_n(s)$. Then the coefficients $\{a_j\}$ and $\{b_j\}$ of polynomials $P_{n-1}(s)$ and $Q_n(s)$ can be computed as follows. Multiplying $Q_n(s)$ on both sides of (10) yields

$$H(s)Q_n(s) = P_{n-1}(s) + \mathcal{O}((s - s_0)^{2n}). \tag{12}$$

Comparing the first n $(s - s_0)^k$ -terms of (12) for $k = 0, 1, \dots, n - 1$ shows that the coefficients $\{b_j\}$ of the denominator polynomial $Q_n(s)$ satisfy the following system of simultaneous equations:

$$\begin{bmatrix} m_0 & m_1 & \dots & m_{n-1} \\ m_1 & m_2 & \dots & m_n \\ \vdots & \vdots & & \vdots \\ m_{n-1} & m_n & \dots & m_{2n-2} \end{bmatrix} \begin{bmatrix} b_n \\ b_{n-1} \\ \vdots \\ b_1 \end{bmatrix} = - \begin{bmatrix} m_n \\ m_{n+1} \\ \vdots \\ m_{2n-1} \end{bmatrix}. \tag{13}$$

The coefficient matrix of (13) is called the *Hankel matrix*, denoted as \mathbf{M}_n . Once the coefficients $\{b_j\}$ are computed, then by comparing the second n $(s - s_0)^k$ -terms of (12) for $k = n, n + 1, \dots, 2n - 1$, we see that the coefficients $\{a_j\}$ of the numerator polynomial $P_{n-1}(s)$ can be computed according to

$$\begin{aligned} a_0 &= m_0 \\ a_1 &= m_0 b_1 + m_1 \\ &\vdots \\ a_{n-1} &= m_0 b_{n-1} + m_1 b_{n-2} + \dots + m_{n-2} b_1 + m_{n-1}. \end{aligned}$$

It is clear that $H_n(s)$ defines a unique n th Padé approximant of $H(s)$ if, and only if, the Hankel matrix \mathbf{M}_n is nonsingular. We will assume that this is the case for all n .

This formulates the framework of the asymptotic waveform evaluation (AWE) techniques as they are known in circuit simulation, first presented in [70] around 1990. The manuscript [20] has a complete treatment of the AWE technique and its variants. A survey of the Padé techniques for model reduction of linear systems is also presented in the earlier work [17]. It is well-known that in practice, the Hankel matrix \mathbf{M}_n is generally extremely ill-conditioned. Therefore, the computation of Padé approximants using explicit moments is inherently numerically unstable. Indeed, this approach can be used only for very small values of n , such as $n \leq 20$, even with some sophisticated schemes to improve the conditioning of the underlying Hankel matrix \mathbf{M}_n . As a result, the approximation range of a computed Padé approximant is limited to only a narrow frequency range around the selected expansion point s_0 . A large number of expansion points is generally required for the approximation of the transfer function $H(s)$ over a broad frequency range of interest. Since for each expansion point s_0 , one has to be concerned with the cost of applying the matrix $\mathbf{A} = -(\mathbf{G} + s_0 \mathbf{C})^{-1} \mathbf{C}$, which is generally the most expensive part of the overall computational cost, one would like to use as few expansion points as possible by increasing the order n of Padé approximants with a selected expansion point s_0 . Fortunately, numerical difficulties associated with explicit moments can be remedied by exploiting the well-known connection between the Padé approximants and the Lanczos process. We will discuss this connection in the next section.

2.4. Krylov subspaces and the Lanczos process

A Krylov subspace is a subspace spanned by a sequence of vectors generated by a given matrix and a vector as follows. Given a matrix \mathbf{A} and a starting vector \mathbf{r} , the n th Krylov subspace $\mathcal{K}_n(\mathbf{A}, \mathbf{r})$ is spanned by a sequence of n column vectors:

$$\mathcal{K}_n(\mathbf{A}, \mathbf{r}) = \text{span}\{\mathbf{r}, \mathbf{A}\mathbf{r}, \mathbf{A}^2\mathbf{r}, \dots, \mathbf{A}^{n-1}\mathbf{r}\}.$$

This is sometimes called the right Krylov subspace. When the matrix \mathbf{A} is nonsymmetric, there is a left Krylov subspace generated by \mathbf{A}^T and a starting vector \mathbf{l} defined by

$$\mathcal{K}_n(\mathbf{A}^T, \mathbf{l}) = \text{span}\{\mathbf{l}, \mathbf{A}^T\mathbf{l}, (\mathbf{A}^T)^2\mathbf{l}, \dots, (\mathbf{A}^T)^{n-1}\mathbf{l}\}.$$

Note that the first $2n$ moments $\{m_j\}$ of $H(s)$ in (9), which define the Hankel matrix \mathbf{M}_n in the Padé approximant (13), are connected with Krylov subspaces through computing the inner products between the left and right Krylov sequences:

$$m_{2j} = ((\mathbf{A}^T)^j \mathbf{l})^T \cdot (\mathbf{A}^j \mathbf{b})^T, \quad m_{2j+1} = ((\mathbf{A}^T)^j \mathbf{l})^T \cdot (\mathbf{A}^{j+1} \mathbf{b})^T,$$

for $j = 1, 2, \dots, n - 1$. Therefore, loosely speaking, the left and right Krylov subspaces contain the desired information of moments, but the vectors $\{A^j \mathbf{r}\}$ and $\{(A^T)^j \mathbf{l}\}$ are unsuitable as basis vectors. The remedy is to construct more suitable basis vectors:

$$\{\mathbf{v}_1, \mathbf{v}_2, \dots, \mathbf{v}_n\} \quad \text{and} \quad \{\mathbf{w}_1, \mathbf{w}_2, \dots, \mathbf{w}_n\},$$

such that they span the same desired Krylov subspaces, specifically, $\mathcal{K}_n(\mathbf{A}, \mathbf{r}) = \text{span}\{\mathbf{v}_1, \mathbf{v}_2, \dots, \mathbf{v}_n\}$ and $\mathcal{K}_n(\mathbf{A}^T, \mathbf{l}) = \text{span}\{\mathbf{w}_1, \mathbf{w}_2, \dots, \mathbf{w}_n\}$. It is well-known that the Lanczos process is an elegant way to generate the desired basis vectors [53]. Given a matrix \mathbf{A} , a right starting vector \mathbf{r} and a left starting vector \mathbf{l} , the Lanczos process generates the desired basis vectors $\{\mathbf{v}_i\}$ and $\{\mathbf{w}_i\}$, known as the *Lanczos vectors*. Moreover, these Lanczos vectors are constructed to be biorthogonal

$$\mathbf{w}_j^T \mathbf{v}_k = 0, \quad \text{for all } j \neq k. \tag{14}$$

The Lanczos vectors can be generated by two three-term recurrences. These recurrences can be stated compactly in matrix form as follows

$$\begin{aligned} \mathbf{A} \mathbf{V}_n &= \mathbf{V}_n \mathbf{T}_n + \rho_{n+1} \mathbf{v}_{n+1} \mathbf{e}_n^T, \\ \mathbf{A}^T \mathbf{W}_n &= \mathbf{W}_n \tilde{\mathbf{T}}_n + \eta_{n+1} \mathbf{w}_{n+1} \mathbf{e}_n^T, \end{aligned}$$

where \mathbf{T}_n and $\tilde{\mathbf{T}}_n$ are the tridiagonal matrices

$$\mathbf{T}_n = \begin{bmatrix} \alpha_1 & \beta_2 & & & \\ \rho_2 & \alpha_2 & \ddots & & \\ & \ddots & \ddots & \beta_n & \\ & & \rho_n & \alpha_n & \end{bmatrix}, \quad \tilde{\mathbf{T}}_n^T = \begin{bmatrix} \alpha_1 & \gamma_2 & & & \\ \eta_2 & \alpha_2 & \ddots & & \\ & \ddots & \ddots & \gamma_n & \\ & & \eta_n & \alpha_n & \end{bmatrix}$$

and they are related by a diagonal similarity transformation $\tilde{\mathbf{T}}_n^T = \mathbf{D}_n \mathbf{T}_n \mathbf{D}_n^{-1}$, where $\mathbf{D}_n = \mathbf{W}_n^T \mathbf{V}_n = \text{diag}(\delta_1, \delta_2, \dots, \delta_k)$. The projection of the matrix \mathbf{A} onto $\mathcal{K}_n(\mathbf{A}, \mathbf{r})$ and orthogonally to $\mathcal{K}_n(\mathbf{A}^T, \mathbf{l})$ is represented by

$$\mathbf{W}_n^T \mathbf{A} \mathbf{V}_n = \mathbf{D}_n \mathbf{T}_n.$$

If the Lanczos process is carried to the end with N being the last step, then it can be viewed as a means of tridiagonalizing \mathbf{A} by a similarity transformation:

$$\mathbf{V}_N^{-1} \mathbf{A} \mathbf{V}_N = \mathbf{T}_N, \tag{15}$$

where \mathbf{T}_N is a tridiagonal matrix, with \mathbf{T}_n as its $n \times n$ leading principal submatrix, $n \leq N$. An algorithm template for the basic Lanczos process is presented in Fig. 1. The Lanczos vectors are determined up to a scaling. We use the scaling $\|\mathbf{v}_j\|_2 = \|\mathbf{w}_j\|_2 = 1$ for all j .

We note that the Lanczos process could stop prematurely due to $\delta_k = 0$ (or $\delta_k \approx 0$ considering the finite precision arithmetic) at step 7 in Fig. 1. This is called *breakdown*. Our assumption of the nonsingularity of the Hankel matrix \mathbf{M}_n guarantees that no breakdown occurs, see [64]. In practice, the problem is curable by a variant of the Lanczos process, for example, a look-ahead scheme is proposed in [33]. An implementation of the Lanczos process with a look-ahead scheme to overcome the breakdown can be found in QMRPACK [35].

-
- (1) $\rho_1 = \|\mathbf{r}\|_2$
 - (2) $\eta_1 = \|\mathbf{I}\|_2$
 - (3) $\mathbf{v}_1 = \mathbf{r}/\rho_1$
 - (4) $\mathbf{w}_1 = \mathbf{I}/\eta_1$
 - (5) **for** $k = 1, 2, \dots, n$ **do**
 - (6) $\delta_k = \mathbf{w}_k^T \mathbf{v}_k$
 - (7) $\alpha_k = \mathbf{w}_k^T \mathbf{A} \mathbf{v}_k / \delta_k$
 - (8) $\beta_k = (\delta_k / \delta_{k-1}) \eta_k$
 - (9) $\gamma_k = (\delta_k / \delta_{k-1}) \rho_k$
 - (10) $\mathbf{v} = \mathbf{A} \mathbf{v}_k - \mathbf{v}_k \alpha_k - \mathbf{v}_{k-1} \beta_k$
 - (11) $\mathbf{w} = \mathbf{A}^T \mathbf{w}_k - \mathbf{w}_k \alpha_k - \mathbf{w}_{k-1} \gamma_k$
 - (12) $\rho_{k+1} = \|\mathbf{v}\|_2$
 - (13) $\eta_{k+1} = \|\mathbf{w}\|_2$
 - (14) $\mathbf{v}_{k+1} = \mathbf{v} / \rho_{k+1}$
 - (15) $\mathbf{w}_{k+1} = \mathbf{w} / \eta_{k+1}$
 - (16) **end for**
-

Fig. 1. Algorithm template for the basic n -step Lanczos process.

2.5. Reduced-order modeling using the Lanczos process

Let us first consider the Lanczos process as a process for tridiagonalizing the matrix \mathbf{A} . Then by (15), the transfer function $H(s)$ of the original system (1) can be rewritten as

$$H(s) = (\mathbf{l}^T \mathbf{r}) \mathbf{e}_1^T (\mathbf{I} - (s - s_0) \mathbf{T}_N)^{-1} \mathbf{e}_1 = (\mathbf{l}^T \mathbf{r}) \frac{\det(\mathbf{I} - (s - s_0) \mathbf{T}'_N)}{\det(\mathbf{I} - (s - s_0) \mathbf{T}_N)} \quad (16)$$

where \mathbf{T}'_N is an $(N - 1) \times (N - 1)$ matrix obtained by deleting the first row and column of \mathbf{T}_N . Note that for the second equality, we have used the following Cauchy–Binet theorem to the matrix $\mathbf{I} - (s - s_0) \mathbf{T}_N$:

$$(\mathbf{I} - (s - s_0) \mathbf{T}_N) \cdot \text{adj}(\mathbf{I} - (s - s_0) \mathbf{T}_N) = \det(\mathbf{I} - (s - s_0) \mathbf{T}_N) \cdot \mathbf{I},$$

where $\text{adj}(\mathbf{X})$ stands for the classical adjugate matrix made up of the $(N - 1) \times (N - 1)$ cofactors of \mathbf{X} . Expression (16) is called the *zero-pole representation*. It is clear that the poles of $H(s)$ can be computed from the eigenvalues of the $N \times N$ tridiagonal matrix \mathbf{T}_N and the zeros of $H(s)$ from the eigenvalues of the $(N - 1) \times (N - 1)$ tridiagonal matrix \mathbf{T}'_N . More precisely, the poles are given by $p_j = s_0 + 1/\lambda_j$, $\lambda_j \in \lambda(\mathbf{T}_N)$, and the zeros by $z_j = s_0 + 1/\lambda'_j$, $\lambda'_j \in \lambda(\mathbf{T}'_N)$.

Now, let us turn to large-scale linear systems where the order N of the matrix \mathbf{A} is too large to fully tridiagonalize, and where the Lanczos process terminates at n ($\leq N$). Then it is natural to define an n th reduced-order approximation of the transfer function $H(s)$ as

$$H_n(s) = (\mathbf{l}^T \mathbf{r}) \mathbf{e}_1^T (\mathbf{I} - (s - s_0) \mathbf{T}_n)^{-1} \mathbf{e}_1, \quad (17)$$

where \mathbf{T}_n is the $n \times n$ leading principal submatrix of \mathbf{T}_N , as generated by the first n steps of the basic Lanczos process outlined in Fig. 1. In analogy to (16), we have the zero-pole representation of $H_n(s)$:

$$H_n(s) = (\mathbf{l}^T \mathbf{r}) \frac{\det(\mathbf{I} - (s - s_0) \mathbf{T}'_n)}{\det(\mathbf{I} - (s - s_0) \mathbf{T}_n)}, \quad (18)$$

where \mathbf{T}'_n is an $(n - 1) \times (n - 1)$ matrix obtained by deleting the first row and column of \mathbf{T}_n .

Now, the question is: what is $H_n(s)$? The answer, which seems surprising to many first-time readers, is that $H_n(s)$ is the Padé approximation of $H(s)$ as computed by using explicit moments in Section 2.3. To show this, let us first recall the following lemma, which was originally developed in [89] for a convergence analysis of the Lanczos algorithm for eigenvalue problems.

Lemma 1. *If T_n is the $n \times n$ leading principal submatrix of T_N , where $n \leq N$. Then for any $0 \leq j \leq 2n - 1$,*

$$\mathbf{e}_1^T T_N^j \mathbf{e}_1 = \mathbf{e}_1^T T_n^j \mathbf{e}_1$$

and for $j = 2n$,

$$\mathbf{e}_1^T T_N^{2n} \mathbf{e}_1 = \mathbf{e}_1^T T_n^{2n} \mathbf{e}_1 + \beta_2 \beta_3 \cdots \beta_n \beta_{n+1} \cdot \rho_2 \rho_3 \cdots \rho_n \rho_{n+1}.$$

A verification of this lemma can be easily carried out by induction. By Lemma 1, we immediately see that the first $2n$ moments of $H(s)$ and $H_n(s)$ are matched:

$$m_j = \mathbf{l}^T \mathbf{A}^j \mathbf{r} = (\mathbf{l}^T \mathbf{r}) \mathbf{e}_1^T T_N^j \mathbf{e}_1 = (\mathbf{l}^T \mathbf{r}) \mathbf{e}_1^T T_n^j \mathbf{e}_1 = \hat{m}_j \quad (19)$$

for $j = 0, 1, \dots, 2n - 1$. Furthermore, by Taylor expansions of $H(s)$ and $H_n(s)$ about s_0 and (19), we have

$$H(s) = H_n(s) + (\mathbf{l}^T \mathbf{r}) \left(\prod_{j=2}^{n+1} \beta_j \prod_{j=2}^{n+1} \rho_j \right) (s - s_0)^{2n} + \mathcal{O}((s - s_0)^{2n+1}).$$

Therefore, we conclude that $H_n(s)$ is a Padé approximant of $H(s)$.

This Lanczos–Padé connection at least goes back to [40] and [41]. The work of [26,37] advocates the use of the Lanczos–Padé connection instead of the mathematical equivalent, but numerically unstable AWE method [70] in the circuit simulation community. The Lanczos-based Padé approximation method has become known as the PVL (Padé Via Lanczos) method, as coined in [26]. An overview of various Krylov methods and their applications in model reduction for state-space control models in control system theory is presented in [13]. The presentation style here partially follows the work of [11]. In the following, we present two examples, one from circuit simulation and one from structural dynamics, as empirical validation of the efficiency of the PVL method. We note that in both cases, we only use one expansion point s_0 over the entire range of frequencies of interest. However, the degree of the underlying Padé approximants constructed via the Lanczos process is as high as 60, which seems to be an impossible mission by using explicit moment-matching as discussed in Section 2.3.

The first example demonstrates the efficiency of the PVL method for a popular circuit problem, which simulates a lumped element network generated by a 3-D electro-magnetic problem modeled via the partial element equivalent circuit (PEEC) model [20,26]. The PEEC model is obtained by appropriate discretizations of the boundary integral formulation of Maxwell’s equations for the electric and magnetic fields at any point in a conductor [73]. The order of the system matrices \mathbf{C} and \mathbf{G} is 306. To capture the dynamic behavior of the transfer function $H(s)$ over the broad frequency range $[\omega_{\min}, \omega_{\max}] = [1, 5 \times 10^9]$, it is necessary to evaluate $H(s)$ at a large number of frequency points. We used a total of 1001 frequency points. On the left of Fig. 2, we plot the absolute values of $H(s)$ and the Padé approximant $H_{60}(s)$ of order 60 generated by the PVL method with only a single expansion $s_0 = 2\pi \times 10^9$. Note that it is nearly indistinguishable from the curve of $|H(s)|$. The right plot of Fig. 2 is the relative error between $H(s)$ and $H_{60}(s)$.

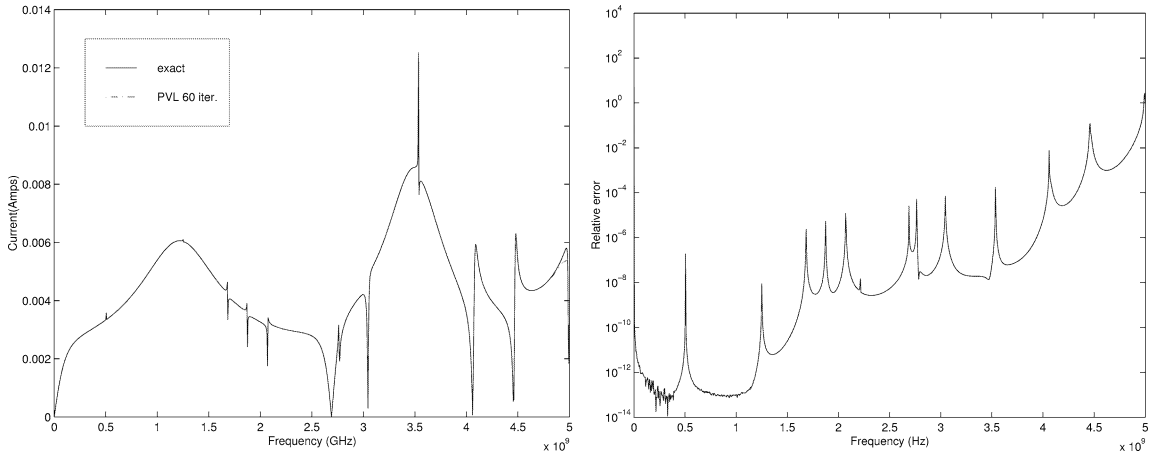


Fig. 2. PEEC example, $|H(s)|$ and PVL $|H_{60}(s)|$ (left) and relative error $|H(s) - H_{60}(s)|/|H(s)|$ (right).

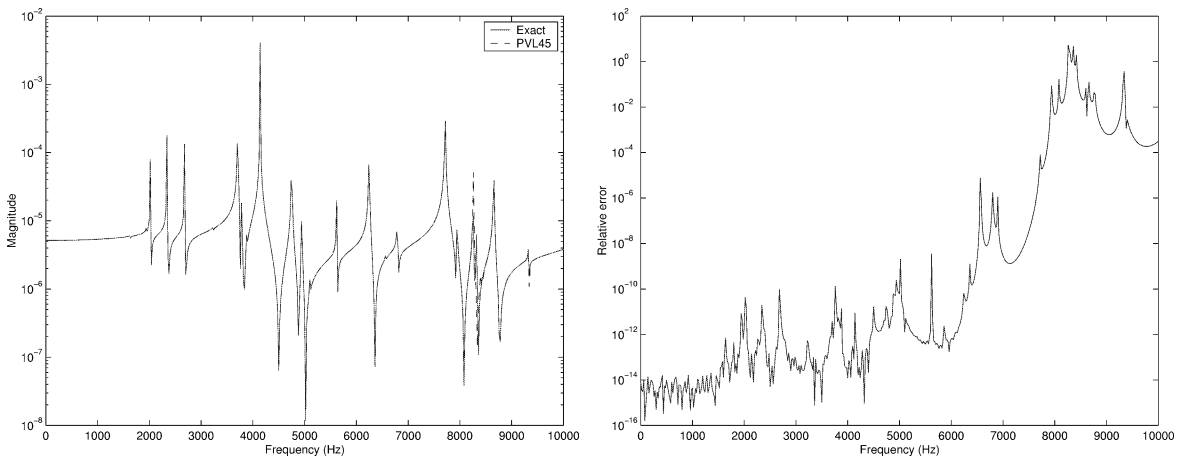


Fig. 3. Automobile brake example, $|H(s)|$ and PVL $|H_{45}(s)|$ (left) and relative error $|H(s) - H_{45}(s)|/|H(s)|$ (right).

The second example is from dynamics analysis of automobile brakes, extracted from MSC/NASTRAN, a finite element analysis software for structural dynamics [50]. The order of the mass matrix \mathbf{M} and stiffness matrix \mathbf{K} is 834. The transfer function is of the form $H(s) = \mathbf{I}^T(\mathbf{K} + s^2\mathbf{M})^{-1}\mathbf{b}$. The expansion point is chosen as $s_0 = 0$. A total of 501 frequency points is evaluated between 0 and 10000 Hz. The left plot of Fig. 3 shows the magnitudes of the original transfer function $H(s)$ and the reduced-order transfer function $H_{45}(s)$ after 45 PVL iterations. The right plot of Fig. 3 shows the relative error between $H(s)$ and $H_{45}(s)$.

2.6. Error estimation

An important question associated with the PVL method is how to determine the order n of a Padé approximant $H_n(s)$, or equivalently, the number of steps of the Lanczos process in order to achieve a desired accuracy of the approximation. In [10], through an algebraic derivation, it is shown that forward

error between the full-order transfer function $H(s)$ and the reduced-order transfer function $H_n(s)$ is given by

$$H(s) - H_n(s) = (\mathbf{l}^T \mathbf{r}) \left(\frac{\rho_{n+1} \eta_{n+1}}{\delta_n} \right) [\sigma^2 \tau_{n1}(\sigma) \tau_{1n}(\sigma)] \gamma_{n+1}(\sigma), \tag{20}$$

where $\sigma = s - s_0$, $\tau_{1n}(\sigma) = \mathbf{e}_1^T (\mathbf{I} - \sigma \mathbf{T}_n)^{-1} \mathbf{e}_n$, $\tau_{n1}(\sigma) = \mathbf{e}_n^T (\mathbf{I} - \sigma \mathbf{T}_n)^{-1} \mathbf{e}_1$, and $\gamma_{n+1}(\sigma) = \mathbf{w}_{n+1}^T (\mathbf{I} - \sigma \mathbf{A})^{-1} \mathbf{v}_{n+1}$. From (20), we see that there are essentially two factors to determine the forward error of the PVL method, namely $\sigma^2 \tau_{n1}(\sigma) \tau_{1n}(\sigma)$ and $\gamma_{n+1}(\sigma)$. Numerous numerical experiments indicate that the first factor, which can be easily computed during the PVL approximation, is the primary contributor to the convergence of the PVL approximation, while the second factor tends to be steady when n increases. Note that $\tau_{n1}(\sigma)$ and $\tau_{1n}(\sigma)$ are the $(1, n)$ and $(n, 1)$ elements of the inverse of the tridiagonal matrix $\mathbf{I} - \sigma \mathbf{T}_n$. This is in agreement with the rapid decay phenomenon observed in the inverse of a band matrix [58]. Fig. 4 shows typical convergence behavior of the factor $|\sigma^2 \tau_{n1}(\sigma) \tau_{1n}(\sigma)|$ for a fixed σ . The direct computation of the second factor $\gamma_{n+1}(\sigma)$ would cost just as much as computing the original transfer function. It is advocated that $\mathbf{w}_{n+1}^T \mathbf{A} \mathbf{v}_{n+1}$ be used as an estimation of the factor $\gamma_{n+1}(\sigma)$ near convergence. With this observation, it is possible to implement the PVL method with an adaptive stopping criteria to determine the required number of Lanczos iterations, see [10]. Related work for error estimation can be found in [48,42] and recently in [62].

More efficient and accurate error estimations of the PVL approximation and its extension to the other moment-matching based Krylov techniques warrant further study. One alternative approach is to use the technique of backward error analysis. By some algebraic derivation, it can be shown that the reduced-order transfer function $H_n(s)$ of (17) can be interpreted as the exact transfer function of a perturbed full-order system. Specifically,

$$H_n(s) = (\mathbf{l}^T \mathbf{r}) \cdot \mathbf{e}_1^T (\mathbf{I} - (s - s_0) \mathbf{T}_n)^{-1} \mathbf{e}_1 = \mathbf{l}^T [\mathbf{I} - (s - s_0) (\mathbf{A} + \mathbf{F}_n)]^{-1} \mathbf{r},$$

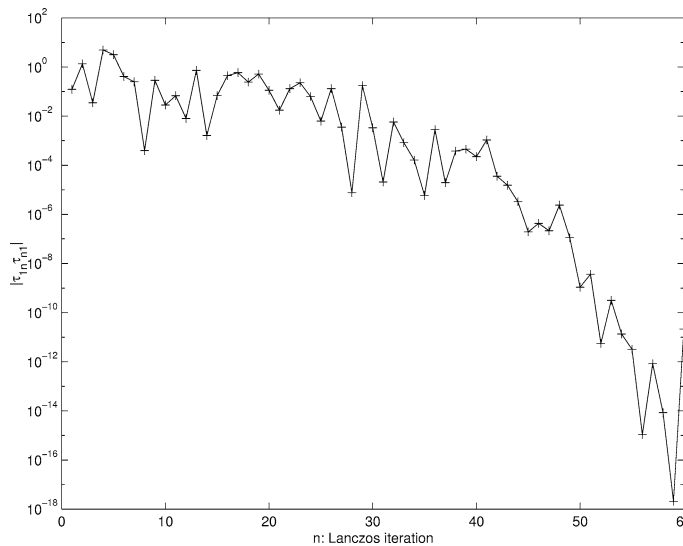


Fig. 4. Convergence of $|\tau_{n1}(\sigma) \tau_{1n}(\sigma)|$ for a fixed $\sigma = s - s_0$.

where

$$\mathbf{F}_n = -\frac{1}{\delta_n} \begin{bmatrix} \mathbf{v}_n & \mathbf{v}_{n+1} \end{bmatrix} \begin{bmatrix} 0 & \eta_{n+1} \\ \rho_{n+1} & 0 \end{bmatrix} \begin{bmatrix} \mathbf{w}_n^T \\ \mathbf{w}_{n+1}^T \end{bmatrix}.$$

Therefore, one may use $\|\mathbf{F}_n\|$ for monitoring convergence. However, it is observed that this is generally a conservative monitor and often does not indicate practical convergence. An open problem is to find an optimal normwise relative backward error

$$\eta(\varepsilon) = \min\{\varepsilon: \mathbf{I}^T[\mathbf{I} - (s - s_0)(\mathbf{A} + \mathbf{F}_n)]^{-1} \mathbf{r} = H_n(s), \|\mathbf{F}_n\| \leq \varepsilon \|\mathbf{A}\|\}.$$

With this optimal backward error and perturbation analysis of the transfer function $H(s)$, one may be able to derive a more efficient error estimation scheme.

2.7. Reduced-order modeling in the time domain

We now show how to construct a reduced-order model of the linear system (1) in the time domain for transient analysis. With a selected expansion point s_0 as for the steady-state analysis, the linear system (1) under the so-called “shift-and-invert” transformation becomes

$$\begin{cases} -\mathbf{A}\dot{\mathbf{x}}(t) + (\mathbf{I} + s_0\mathbf{A})\mathbf{x}(t) = \mathbf{r}u(t), \\ \mathbf{y}(t) = \mathbf{I}^T\mathbf{x}(t), \end{cases}$$

where $\mathbf{A} = -(\mathbf{G} + s_0\mathbf{C})^{-1}\mathbf{C}$ and $\mathbf{r} = (\mathbf{G} + s_0\mathbf{C})^{-1}\mathbf{b}$. Let \mathbf{V}_n be the Lanczos vectors generated by the Lanczos process with matrix \mathbf{A} and starting vectors \mathbf{r} and \mathbf{l} as discussed in Section 2.4. Then considering the approximation of the state vector $\mathbf{x}(t)$ by another state vector, constrained to stay in the subspace spanned by the columns of \mathbf{V}_n , namely,

$$\mathbf{x}(t) \approx \mathbf{V}_n\mathbf{z}(t) \quad \text{for some } \mathbf{z}(t) \in \mathcal{R}^N,$$

yields an over-determined linear system with respect to the state variable $\mathbf{z}(t)$:

$$\begin{cases} -\mathbf{A}\mathbf{V}_n\dot{\mathbf{z}}(t) + (\mathbf{I} + s_0\mathbf{A})\mathbf{V}_n\mathbf{z}(t) = \mathbf{r}u(t), \\ \tilde{\mathbf{y}}(t) = \mathbf{I}^T\mathbf{V}_n\mathbf{z}(t). \end{cases}$$

After left-multiplying the first equation by \mathbf{W}_n^T , we have

$$\begin{cases} -\mathbf{W}_n^T\mathbf{A}\mathbf{V}_n\dot{\mathbf{z}}(t) + \mathbf{W}_n^T(\mathbf{I} + s_0\mathbf{A})\mathbf{V}_n\mathbf{z}(t) = \mathbf{W}_n^T\mathbf{r}u(t), \\ \tilde{\mathbf{y}}(t) = \mathbf{I}^T\mathbf{V}_n\mathbf{z}(t). \end{cases}$$

Then an n th reduced-order model of the linear system (1) in the time domain is naturally defined as

$$\begin{cases} \mathbf{C}_n\dot{\mathbf{z}}(t) + \mathbf{G}_n\mathbf{z}(t) = \mathbf{r}_n u(t), \\ \tilde{\mathbf{y}}(t) = \mathbf{I}_n^T\mathbf{z}(t), \end{cases} \quad (21)$$

where

$$\mathbf{C}_n = -\mathbf{W}_n^T\mathbf{A}\mathbf{V}_n, \quad \mathbf{G}_n = \mathbf{W}_n^T(\mathbf{I} + s_0\mathbf{A})\mathbf{V}_n, \quad \mathbf{r}_n = \mathbf{W}_n^T\mathbf{r} \quad \text{and} \quad \mathbf{I}_n = \mathbf{V}_n^T\mathbf{l}.$$

By using the governing equations of the Lanczos process presented in Section 2.4, the quadruples $(\mathbf{C}_n, \mathbf{G}_n, \mathbf{r}_n, \mathbf{I}_n)$ can be simply expressed as $\mathbf{C}_n = -\mathbf{T}_n$, $\mathbf{G}_n = (\mathbf{I}_n - s_0\mathbf{T}_n)$, $\mathbf{r}_n = \rho_1\mathbf{e}_1$, and $\mathbf{I}_n = \eta_1\delta_1\mathbf{e}_1$.

Fig. 5 shows the PVL method for transient analysis of a small RLC network presented in [20, p. 29]. The system matrices \mathbf{C} and \mathbf{G} have order 11. An input excitation $u(t)$ of 0.1 ns rise/fall and 0.3 ns duration

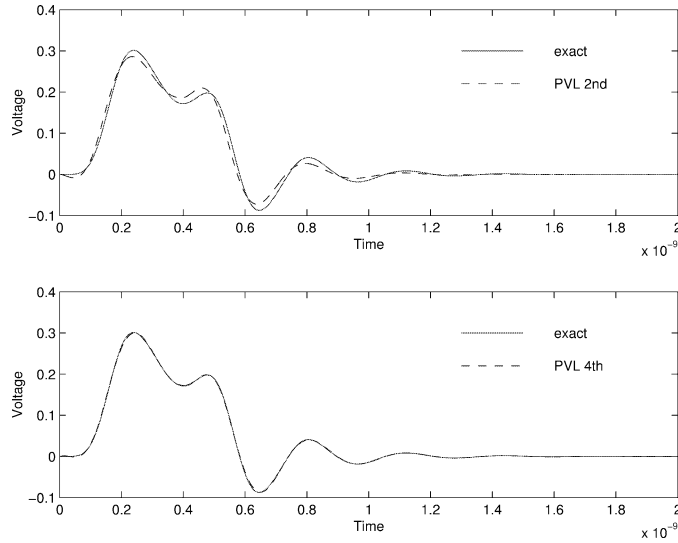


Fig. 5. RLC network transient responses: 2nd and 4th order PVL approximation.

was simulated. The convergence for orders 2 and 4 of the reduced-order models in the time domain is shown in Fig. 5. The expansion point is chosen to be $s_0 = \pi \times 10^9$. In this example, we have observed the discrepancy between the rate of convergence of the frequency response and transient response. The relationship between convergence of the frequency response and transient response is a subject of further study.

2.8. Stability and passivity

In this section, we discuss two essential properties associated with the linear dynamical system (1), namely stability and passivity. One question is whether or not the tendency of the system response to grow or decay in time characterizes the system's stability. The second question is whether or not the system's capability of generating energy from sources used to excite it characterizes the system's passivity. For the linear system (1), stability can be formally defined via the poles of the transfer function $H(s)$.

Definition 2. A linear(ized) system is *stable*

- if all the poles p_j of $H(s)$ lie in $\mathcal{C}_- := \{s \in \mathcal{C} \mid \Re(s) < 0\}$ and
- if all the poles p_j of $H(s)$ on the imaginary axis, $\Re(p_j) = 0$, are simple.

A stable system guarantees a bounded response to a bounded input, see for example, [2]. If the linear dynamical system (1) describes an actual physical system, such as a functioning electronic circuit, then it will necessarily be stable. Note that for the transfer function $H(s)$ given by (5), any pole p_j is of the form $p_j = s_0 + 1/\lambda_j$, where $\lambda_j \in \lambda(\mathbf{A})$. However, in general, not every p_j of the above form is a pole of $H(s)$. Indeed, the poles of $H(s)$ are given by the above form if, and only if, the triple $\{\mathbf{A}, \mathbf{r}, \mathbf{l}\}$ in (5) is a minimal realization of $H(s)$. Recall that for a given transfer function $H(s)$, a representation (5) is called a minimal realization if the state-space dimension N is minimal. Assuming that (5) is a minimal

realization, then the task of verifying whether the full-system system and its reduced-order system are stable becomes the problem of computing eigenvalues of matrices A and T_n .

In an actual physical system, the property of passivity is guaranteed by the physical elements of the system, for example, a linear RLC circuit is always passive. Mathematically, a passive system is defined by

$$\int_0^T y(t) \cdot u(t) dt \geq 0, \quad \forall T \geq 0.$$

For a time-invariant linear dynamical system (1), passivity is equivalent to the positive realness of the associated transfer function $H(s)$.

Definition 3. A function $f: \mathcal{C} \mapsto \mathcal{C} \cup \{\infty\}$ is called *positive real* if

- (1) f is analytic in $\mathcal{C}_+ \equiv \{s \in \mathcal{C}, \Re(s) > 0\}$;
- (2) $f(\bar{s}) = \overline{f(s)}$ for all $s \in \mathcal{C}$;
- (3) $\Re(f(s)) \geq 0$ for all $s \in \mathcal{C}_+$.

Using standard results from complex analysis, such as the maximum modulus theorem, one readily obtains the following well-known conditions for the transfer function $H(s)$ to be positive real.

Theorem 4. The transfer function $H(s)$ of a SISO time-invariant linear dynamical system is said to be *passive* if

- (1) $H(s)$ has no poles in \mathcal{C}_+ ;
- (2) $H(\bar{s}) = \overline{H(s)}$ for all $s \in \mathcal{C}$;
- (3) $\Re(H(i\omega)) \geq 0$ for all $\omega \in \mathcal{R}$.

Note that condition (2) is always satisfied since the quadruples $\{C, G, b, l\}$ in (1) are assumed to be real. Condition (1) can be checked by computing the eigenvalues of the matrix A as given in (5). In view of (1), a passive linear dynamical system is necessarily stable. In [6], it is shown how condition (3) can be checked via computing the eigenvalues of a certain matrix pencil derived from the representation of $H(s)$. In particular, condition (3) implies that all zeros of $H(s)$ must also in \mathcal{C}_- .

Passivity (and positive realness) is a very important concept in system and control theory. Since the introduction of the concept of positive realness by Brune [16] in 1931, there is a large volume of work concerned with characterizing and testing the positive realness. A history and summary of these works can be found in [2,14] and references therein. It is described as an evergreen research topic. The eigenvalue-based characterization and test for positive realness for a SISO transfer function [6] is developed for the applications associated with the reduced-order modeling techniques. Recent related work includes [38,56].

2.9. Post-processing for stability and passivity

It is well-known that when applied to stable and passive linear dynamical systems, reduced-order modeling techniques based on Padé approximation in general do not preserve the stability and passivity

of the original system. For some applications, such as the use of Padé-based reduced-order models for efficient computation of the frequency response, the possible occurrence of unstable poles is not an issue [26]. However, a reduced-order model is often used to replace a large linear subsystem in a stable and passive nonlinear system to reduce the complexity of the simulation of the overall system. In this context, it is crucial that the reduced-order models of the linear subsystems are stable and passive in order to ensure stability of the coupled systems.

In [7], a post-processing technique for the PVL method is proposed to modify the n th order Padé approximant $H_n(s)$ to make it stable, and if the original system is passive, also passive. The resulting variant of the PVL method is called the PVL π method. The following is an outline of the PVL π procedure:

- (1) Run n steps of the PVL to obtain an n th Padé approximant

$$H_n(s) = (\mathbf{l}^T \mathbf{r}) \mathbf{e}_1^T (\mathbf{I} - (s - s_0) \mathbf{T}_n)^{-1} \mathbf{e}_1 = (\mathbf{l}^T \mathbf{r}) \frac{\det(\mathbf{I} - (s - s_0) \mathbf{T}'_n)}{\det(\mathbf{I} - (s - s_0) \mathbf{T}_n)}.$$

- (2) Check stability by computing poles of $H_n(s)$ via eigenvalues of \mathbf{T}_n .
- (3) If passivity is desired, check zeros of $H_n(s)$ via eigenvalues of \mathbf{T}'_n .
- (4) If $H_n(s)$ has poles and/or zeros in \mathcal{C}_+ , then move these unstable poles and zeros into the left half of the complex plane through a rank-one updating of \mathbf{T}_n , subsequently, we have a modified Padé approximant

$$\widehat{H}_n(s) = (\mathbf{l}^T \mathbf{r}) \mathbf{e}_1^T (\mathbf{I} - (s - s_0) \widehat{\mathbf{T}}_n)^{-1} \mathbf{e}_1$$

where $\widehat{\mathbf{T}}_n = \mathbf{T}_n + \text{“rank-one update”}$.

- (5) If $\widehat{H}_n(s)$ has no more poles in \mathcal{C}_+ , then $\widehat{H}_n(s)$ is stable.
- (6) If $\widehat{H}_n(s)$ has neither poles nor zeros in \mathcal{C}_+ , then $\widehat{H}_n(s)$ satisfies the necessary condition for passivity.
- (7) Check the remaining sufficient condition $\Re(\widehat{H}_n(j\omega)) \geq 0$ for all $\omega \in \mathcal{R}$ for passivity of $\widehat{H}_n(s)$ via the criterion developed in [6].

By the proper rank-one update of \mathbf{T}_n , we are not only able to move unstable poles and/or zeros, but also are able to show that

$$\widehat{H}_n(s) = H(s) + \mathcal{O}((s - s_0)^{2n-m}),$$

where $m = \ell + k$, corresponds to the ℓ zeros and k poles to be moved. This implies that PVL π treats the accuracy of Padé approximation for stability and passivity. Unfortunately, we are not aware of a systematic way of choosing prescribed positions in the left half of the complex plane for unstable poles and/or zeros to be moved to so that it is guaranteed that all poles and zeros of the modified Padé approximant $\widehat{H}_n(s)$ are stable, and meanwhile there is the least loss of moments matched. PVL π is a *trial-and-error* procedure. It might be necessary to repeat steps (4) to (7) for a different set of positions for the unstable poles and/or zeros. In the following example, a strategy is proposed to move unstable poles.

This example is a continuation of the PEEC circuit as presented in Section 2.5 and is reported earlier in [7]. With the proper formulation, the circuit is stable with all poles of $H(s)$ in the left half of the complex plane. The PVL method with 60 iterations produces the frequency response $H_{60}(s)$ within the admissible error (see Fig. 2). However, the Padé approximant $H_{60}(s)$ is not stable due to 15 unstable

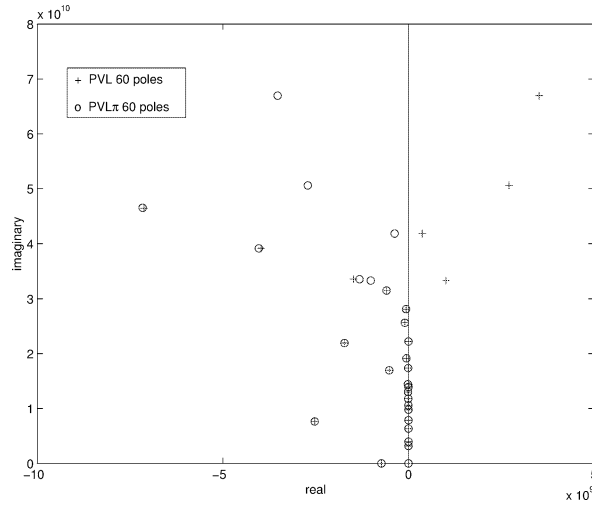


Fig. 6. $H_{60}(s)$ poles (“+”) by PVL and $\widehat{H}_{60}(s)$ poles (“o”) by PVL π .

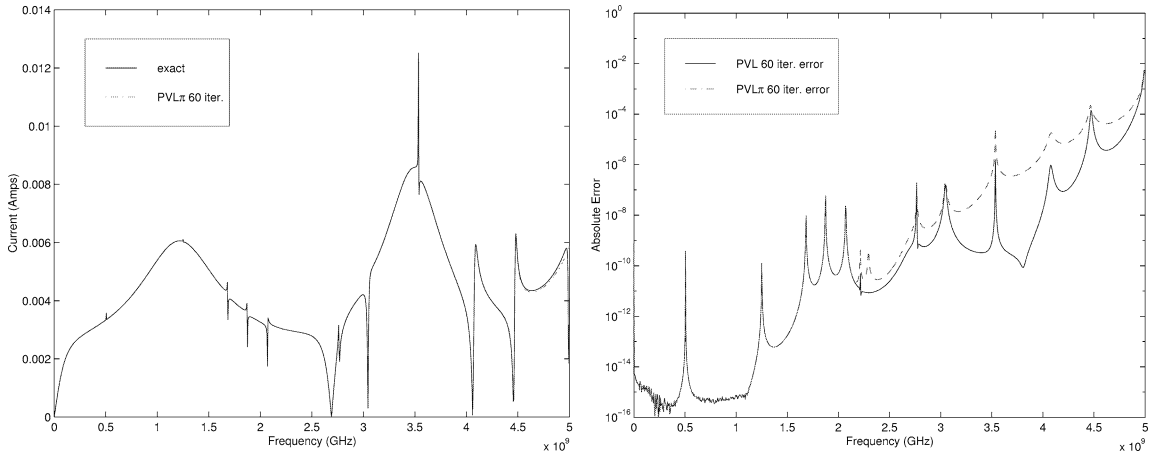


Fig. 7. PVL π approximation (left), and errors $|H(s) - H_n(s)|$ (PVL) and $|H(s) - \widehat{H}_n(s)|$ (PVL π) (right).

poles in the right half plane. Using PVL π , we move unstable poles to stable ones by simply reflecting unstable poles with respect to the imaginary axis and obtain a stable partial Padé approximant $\widehat{H}_{60}(s)$ (see Fig. 6). The left plot of Fig. 7 shows the curves $|H(s)|$ and $|\widehat{H}_{60}(s)|$, and the right plot shows error curves $|H(s) - H_n(s)|$ (PVL) and $|H(s) - \widehat{H}_n(s)|$ (PVL π), for the relevant frequency range. The error curves show that the accuracy of the stable reduced-order transfer function $\widehat{H}_{60}(60)$ remains satisfactory.

There are three ingredients in the PVL π method. The first is the intimate connection between the Lanczos process and formal orthogonal polynomials, see for example [33]. In fact, each pair of right and left Lanczos vectors can be expressed in the form $\mathbf{v}_j = \xi_j \psi_{j-1}(\mathbf{A}) \mathbf{r}$ and $\mathbf{w}_j = \eta_j \psi_{j-1}(\mathbf{A}^T) \mathbf{l}$, where ψ_{j-1} is a monic polynomial of degree $j - 1$ and $\xi_j, \eta_j \neq 0$ are suitable scaling factors. The bi-orthogonality (14) of the Lanczos vectors is equivalent to the formal orthogonality

$$\langle \psi_j, \psi_k \rangle := \mathbf{l}^T \psi_j(\mathbf{A}) \psi_k(\mathbf{A}) \mathbf{r} = 0 \quad \text{for all } j \neq k = 0, 1, \dots, n,$$

of the polynomials $\psi_0, \psi_1, \dots, \psi_n$. The second ingredient is that in analogy to the zero-pole representation (18) of $H_n(s)$, the modified transfer function $\widehat{H}_n(s)$ can be expressed as a rational function of the form

$$\widehat{H}_n(s) = \frac{\psi_{n-1-\ell}(s)}{\varphi_{n-k}(s)} \cdot \frac{\widetilde{\psi}_\ell(s)}{\widetilde{\varphi}_k(s)}$$

where $\widetilde{\psi}_\ell(s)$ and $\widetilde{\varphi}_k(s)$ are fixed polynomials whose roots are the prescribed ℓ zeros and k poles, respectively. The parameters of the polynomials $\psi_{n-1-\ell}(s)$ and $\varphi_{n-k}(s)$ are free. These parameters are chosen such that the first $2n - m$ moments of $H(s)$ and $\widehat{H}_n(s)$ are matched. A rational function of this form is called a *partial Padé approximation* as proposed in [15]. Finally, this partial Padé approximation of the transfer function $H(s)$ can be interpreted as a partial inverse eigenvalue problem, namely, find a vector z such that partial eigenvalues of

$$\widehat{T}_n = T_n + z e_n^T \quad \text{and} \quad \widehat{T}'_n = T'_n + z' e_{n-1}^T$$

are prescribed. This rank-one updating strategy generalizes methods proposed in [39] on computation of certain Gaussian-type quadratures.

2.10. Reduced-order modeling in finite precision

In this section, we discuss the robustness issue of the reduced-order modeling techniques in the presence of finite-precision arithmetic. We examine an important special case of the linear dynamical system (1) where the system matrices C and G are symmetric and positive semidefinite, and the input and output distribution arrays B and L are identical. For example, by employing so-called modified nodal analysis, a linear circuit with only resistors and capacitors (an RC circuit) results in such a system. It can be shown that such a system is automatically stable and passive. Assume $G + s_0 C$ is positive definite for a selected expansion point s_0 . Let $G + s_0 C = M M^T$ be the Cholesky factorization of $G + s_0 C$. Then the associated transfer function can be written as

$$Z(s) = B^T (G + sC)^{-1} B = \widetilde{B}^T (I + (s - s_0)A)^{-1} \widetilde{B},$$

where $A = M^{-1} C M^{-T}$ and $\widetilde{B} = M^{-1} B$. To exploit the symmetry of the transfer function $Z(s)$, we can use a symmetric band Lanczos process, as proposed in [75,28]. Given $A^T = A$ and m starting vectors $\widetilde{B} = \widetilde{Q}_1 = [\widetilde{q}_1 \quad \widetilde{q}_2 \quad \dots \quad \widetilde{q}_m]$, an n -step symmetric band Lanczos process generates a sequence of linearly independent *Lanczos vectors* $Q_n = [q_1 \quad q_2 \quad \dots \quad q_n]$, such that they span the same subspace as the first n linearly independent columns of the Krylov space

$$\mathcal{K}_N(A, \widetilde{Q}_1) = \text{span}\{\widetilde{Q}_1, A \widetilde{Q}_1, A^2 \widetilde{Q}_1, \dots, A^{N-1} \widetilde{Q}_1\}.$$

The Lanczos vectors $\{q_i\}$ can be computed recursively from the following governing relations

$$A Q_n = Q_n \widehat{T}_n + [0 \quad \dots \quad 0 \quad \hat{q}_{n+1} \quad \dots \quad \hat{q}_{n+m_c}] + Q_n^{\text{df}}$$

with the orthogonality conditions $Q_n^T Q_n = I_n$ and $Q_n^T [\hat{q}_{n+1} \quad \dots \quad \hat{q}_{n+m_c}] = \mathbf{0}$, where $m_c (\leq m)$ is the current blocksize due to the possible deflation in $\mathcal{K}_N(A, \widetilde{Q}_1)$. The matrix Q_n^{df} consists of deflated vectors such that $\|Q_n^{\text{df}}\| \leq \tau$ for a given deflation tolerance value τ . The representation of the projection of A onto the Krylov subspace $\text{span}\{Q_n\}$ is given by

$$T_n = Q_n^T A Q_n.$$

As in the classical Lanczos process, the symmetric band Lanczos process generates the entries of T_n directly. Therefore, after n steps of the symmetric band Lanczos process, a reduced-order transfer function of dimension n is defined as follows:

$$Z_n(s) = R_n^T (I_n + (s - s_0)T_n)^{-1} R_n,$$

where $R_n = Q_n^T \tilde{B}$. This is referred to as the SyMPVL method to denote a symmetric matrix Padé approximation via Lanczos process [32]. Since A is positive semidefinite, T_n is also positive semidefinite. As a result, in exact arithmetic, the reduced-order model $Z_n(s)$ is stable and passive. It inherits the essential properties of the original full-order model.

However, in the presence of finite precision arithmetic, roundoff may cause the computed projection T_n of A to be indefinite. Consequently, the reduced-order transfer function $Z_n(s)$ may be unstable and non-passive. For example, Fig. 8 shows the dominant poles of $Z(s)$ for an extracted RC circuit, where C and G are matrices of order $N = 1346$, and the number of inputs (and outputs) is $m = 10$. SyMPVL produces a reduced-order model with admissible error after $n = 60$ iterations. The dominant poles of the original model are all stable, as shown in the third plot of Fig. 8. However, the reduced-order transfer function $Z_n(s)$ has unstable dominant poles, see the first plot in Fig. 8. For analysis and synthesis of such a linear system, positive semi-definiteness of T_n is necessary. This robustness issue of numerical methods in the presence of finite-precision arithmetic arises repeatedly in practical applications. Robustness is vital for an industrial-strength numerical method and its software.

In [8], a remedy is proposed to replace the symmetric band Lanczos process as used in SyMPVL by a mathematically equivalent process but based on a suitably coupled Lanczos process such that it generates the LDL^T factors of T_n , instead of T_n itself. In this way, we can enforce (or verify) positive semi-definiteness of T_n directly. In a compact matrix form, the Lanczos-type process with coupled recurrence can be stated as

$$AP_n = V_n L_n D_n + [0 \quad \dots \quad 0 \quad \tilde{v}_{n+1} \quad \dots \quad \tilde{v}_{n+m_c}] + V_n^{df}, \tag{22}$$

$$V_n = P_n U_n \tag{23}$$

with the following orthogonality conditions:

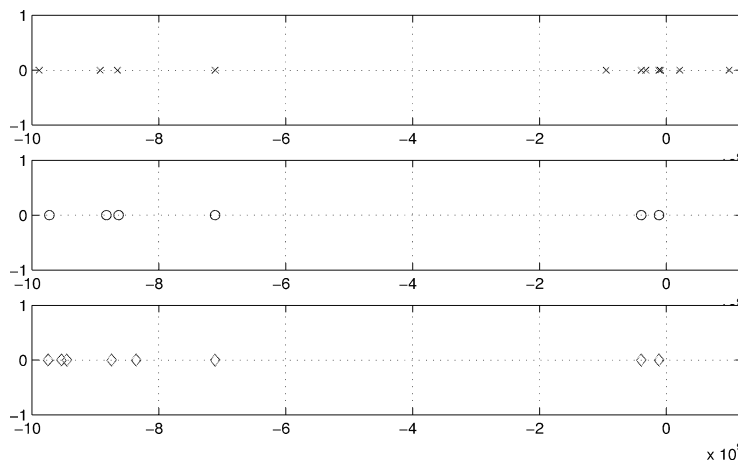


Fig. 8. Dominant poles of a RC circuit (bottom), computed by SyMPVL (top) and SyMPVL2 (middle).

$$\mathbf{V}_n^T \mathbf{V}_n = \mathbf{I}_n, \tag{24}$$

$$\mathbf{V}_n^T [\tilde{\mathbf{v}}_{n+1} \ \dots \ \tilde{\mathbf{v}}_{n+m_c}] = \mathbf{0}, \tag{25}$$

$$\mathbf{P}_n^T \mathbf{A} \mathbf{P}_n = \mathbf{D}_n = \text{diag}(\mathbf{p}_1^T \mathbf{A} \mathbf{p}_1, \mathbf{p}_2^T \mathbf{A} \mathbf{p}_2, \dots, \mathbf{p}_n^T \mathbf{A} \mathbf{p}_n), \tag{26}$$

where \mathbf{L}_n and \mathbf{U}_n are lower and upper triangular matrices, respectively. \mathbf{V}_n consists of Lanczos vectors, \mathbf{P}_n auxiliary vectors and \mathbf{V}_n^{df} deflation vectors.

By multiplying (26) from the left by \mathbf{U}_n^T and from the right by \mathbf{U}_n , and by using (23), it follows that the representation of the projection of \mathbf{A} onto the Krylov subspace spanned by the Lanczos vectors \mathbf{V}_n is given by

$$\mathbf{T}_n = \mathbf{V}_n^T \mathbf{A} \mathbf{V}_n = \mathbf{U}_n^T \mathbf{D}_n \mathbf{U}_n.$$

Thus, the factors \mathbf{U}_n and \mathbf{D}_n of the LDL^T factorization of the projection matrix \mathbf{T}_n are directly computed in this coupled recurrence based Lanczos process. The positive definiteness of \mathbf{T}_n is ensured by the diagonal entries $\{\mathbf{p}_i^T \mathbf{A} \mathbf{p}_i\}$ of \mathbf{D}_n . Subsequently, a reduced-order transfer function of dimension n is defined as

$$\mathbf{Z}_n^{(c)}(s) = \mathbf{R}_n^T (\mathbf{I}_n + (s - s_0) \mathbf{U}_n^T \mathbf{D}_n \mathbf{U}_n)^{-1} \mathbf{R}_n,$$

where $\mathbf{R}_n^T = \mathbf{V}_n^T \tilde{\mathbf{B}}$. This is called the SyMPVL2 method in [8], as a modified version of SyMPVL. The middle plot of Fig. 8 shows the dominant poles computed by SyMPVL2. The diagonal entries of \mathbf{D}_n generated by SyMPVL2 are all positive, and the matrix $\mathbf{U}_n^T \mathbf{D}_n \mathbf{U}_n$ is positive definite. Another desirable by-product of SyMPVL2 is that, for the same dimension n , the reduced-order transfer function $\mathbf{Z}_n^{(c)}(s)$ is typically more accurate as illustrated in Fig. 9.

Finally, we remark that, in a different context, the benefit of using a coupled, instead of a non-coupled, Lanczos process was also noted and exploited in [34,44]. The technique of directly computing the factorized form of a solution is also shown in other applications, such as solving a stable and non-negative definite Lyapunov matrix equation of the form $\mathbf{A}\mathbf{X} + \mathbf{X}\mathbf{A}^T = -\mathbf{C}$, where \mathbf{A} is stable, and \mathbf{C} is positive semidefinite. It is known that the solution \mathbf{X} is positive semidefinite, namely \mathbf{X} can be represented as $\mathbf{X} = \mathbf{L}\mathbf{L}^T$. In [45], it is shown how to directly compute the Cholesky factor \mathbf{L} of \mathbf{X} , instead of \mathbf{X} .

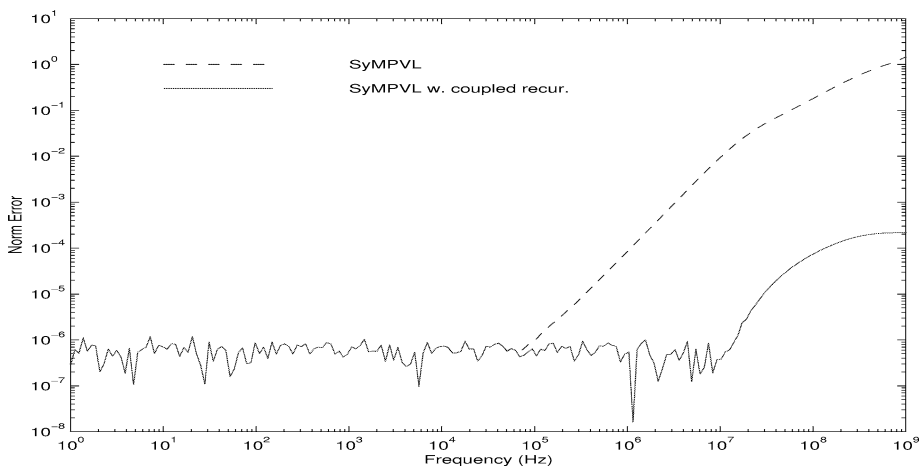


Fig. 9. Accuracy: $\|\mathbf{Z}(s) - \mathbf{Z}_n(s)\|$ vs. $\|\mathbf{Z}(s) - \mathbf{Z}_n^{(c)}(s)\|$.

Another example is to compute eigenvalues of a tridiagonal matrix T in high relative precision. As shown in recent work [65], it is better to work with the LDL^T form of T , instead of T directly. Those efforts highlight ingenuity in the work of numerical analysis and scientific computing.

2.11. *Other reduced-order modeling methods and software availability*

So far, we have focused on the Lanczos-based Krylov subspace techniques with the property of moment-matching for reduced-order modeling of the linear dynamical system (1). Among the early work in this class of methods, besides the aforementioned, we would like to highlight the work of De Villemagne and Skelton [25] in 1987. In this paper, a methodology that exploits the notion of an oblique projection is studied. It has flexibility to allow the reduced-order model to match various combinations of different types of parameters of the full-order model, such as lower frequency ($s_0 = 0$) and high frequency ($s_0 = \infty$) moments. It also contains an up to date list of papers on model reduction techniques. In engineering applications of Krylov subspace based reduced-order model techniques, the works of Nour-Omid and Clough [61] (1984) and Craig, Jr. and Hale [24] (1988) in structural dynamics are among the earliest ones we are aware of.

We have mostly discussed the treatment of single-input single-output systems. A generalization of the PVL method for multi-input multi-output systems is reviewed in [31]. Naturally, it is called the MPVL method since it is based on a Lanczos-type process for multiple starting vectors. Besides Lanczos process based methods, Arnoldi process based methods have also been studied extensively. In [43], an implicitly restarted Lanczos method was developed. In [42], a rational Krylov subspace based method was proposed. For RLC, PRIMA is also widely accepted in the circuit simulation community, which combines the Arnoldi process and a direct orthogonal projection [63]. The connection between PRIMA and SyMPVL is explained in [29].

All moment-matching methods involve local approximations in nature. There is a class of global approximation methods, mostly based on the theory of balanced realization [59]. They sometimes are also called Gramian-based model reduction methods, or SVD-based model reduction methods [86,3]. The crux of this class of methods for applying to large-scale linear dynamical systems lies in solving two large-scale Lyapunov matrix equations for the system gramians. Low rank approximations to the system gramians have been proposed by using Lanczos and Arnoldi-based Krylov subspace techniques in [48, 47]. In the latest work [82], a low rank approximation to a cross gramian is proposed which overcomes the possible inconsistency by solving system gramians independently. Besides Krylov subspace based techniques, ADI based methods for solving the underlying Lyapunov equations are also presented in the recent work [67,55].

In contrast to the vast amount of literature on Krylov-subspace based methods for reduced-order modeling, there is little software available in the public domain. To the knowledge of the author, the PVL method and its variants, and PRIMA have become kernels of proprietary CAD tools for interconnect analysis and other applications in circuit simulation. On the other hand, it is not too hard for readers to implement a Krylov-subspace based reduced-order modeling method, since a major part of the work is based on implementation of Lanczos or Arnoldi processes or their variants. Algorithm templates and their software for these processes can be found in [4] and references therein. In an effort to exchange software and test data for studying, comparing and benchmarking various numerical methods, the author has put a set of Matlab codes which implement the basic Lanczos-based method as outlined in this section at the

web site <http://www.cs.ucdavis.edu/~bai>. In addition, a few test data sets, such as the widely used PEEC example, are also available at this site.

3. Second-order dynamical systems

Second-order models arise naturally in the study of many types of physical systems, with common examples being electrical, mechanical and structural dynamical systems. A time-invariant multi-input multi-output second-order system is described by

$$\begin{cases} \mathbf{M}\ddot{\mathbf{q}}(t) + \mathbf{D}\dot{\mathbf{q}}(t) + \mathbf{K}\mathbf{q}(t) = \mathbf{P}\mathbf{u}(t), \\ \mathbf{y}(t) = \mathbf{E}^T\mathbf{q}(t), \end{cases} \quad (27)$$

with initial conditions $\mathbf{q}(0) = \mathbf{q}_0$ and $\dot{\mathbf{q}}(0) = \dot{\mathbf{q}}_0$. Here t is the time variable, $\mathbf{q}(t) \in \mathcal{R}^N$ is a vector of state variables, $\mathbf{u}(t) \in \mathcal{R}^m$ the input force vector, and $\mathbf{y}(t) \in \mathcal{R}^p$ the output measurement vector. \mathbf{M} , \mathbf{D} , $\mathbf{K} \in \mathcal{R}^{N \times N}$ are system matrices, such as mass, damping and stiffness matrices as they are called in structural dynamics. $\mathbf{P} \in \mathcal{R}^{N \times m}$ is an input distribution array, $\mathbf{E} \in \mathcal{R}^{N \times p}$ is an output measurement array. N is the state-space dimension. m and p are the number of inputs and outputs, respectively. In most practical cases, m and p are much smaller than N .

The second-order system (27) can be reformulated into an equivalent linear system of the form (1) in many different ways. We will use the following linear system equivalent to (27):

$$\begin{cases} \mathbf{C}\dot{\mathbf{x}}(t) + \mathbf{G}\mathbf{x}(t) = \mathbf{B}\mathbf{u}(t), \\ \mathbf{y}(t) = \mathbf{L}^T\mathbf{x}(t), \end{cases} \quad (28)$$

with

$$\mathbf{x}(t) = \begin{bmatrix} \mathbf{q}(t) \\ \dot{\mathbf{q}}(t) \end{bmatrix}, \quad \mathbf{C} = \begin{bmatrix} \mathbf{D} & \mathbf{M} \\ \mathbf{W} & \mathbf{0} \end{bmatrix}, \quad \mathbf{G} = \begin{bmatrix} \mathbf{K} & \mathbf{0} \\ \mathbf{0} & -\mathbf{W} \end{bmatrix}, \quad \mathbf{B} = \begin{bmatrix} \mathbf{P} \\ \mathbf{0} \end{bmatrix}, \quad \mathbf{L} = \begin{bmatrix} \mathbf{E} \\ \mathbf{0} \end{bmatrix},$$

where \mathbf{W} can be any $N \times N$ nonsingular matrix. A common choice of \mathbf{W} is to be the identity matrix, $\mathbf{W} = \mathbf{I}$. If \mathbf{M} , \mathbf{D} and \mathbf{K} are all symmetric and \mathbf{M} is nonsingular, as often occurs in structural dynamics, we can choose $\mathbf{W} = \mathbf{M}$. The result is that \mathbf{C} and \mathbf{G} in the linearized system (28) are symmetric matrices. The symmetry of the original system is preserved.

Assume that for simplicity, we have zero initial conditions $\mathbf{q}(0) = \mathbf{q}_0 = \mathbf{0}$, $\dot{\mathbf{q}}(0) = \dot{\mathbf{q}}_0 = \mathbf{0}$ and $\mathbf{u}(0) = \mathbf{0}$ in (27). Taking the Laplace transform (2) of the second-order system (27), we have

$$\begin{cases} s^2\mathbf{M}\mathbf{Q}(s) + s\mathbf{D}\mathbf{Q}(s) + \mathbf{K}\mathbf{Q}(s) = \mathbf{P}\mathbf{U}(s), \\ \mathbf{Y}(s) = \mathbf{E}^T\mathbf{Q}(s). \end{cases} \quad (29)$$

Eliminating $\mathbf{Q}(s)$ in (29) results in the frequency domain input-output relation $\mathbf{Y}(s) = \mathbf{H}(s)\mathbf{U}(s)$, where $\mathbf{H}(s)$ is the $p \times m$ matrix-valued *transfer function*, given by

$$\mathbf{H}(s) = \mathbf{E}^T(s^2\mathbf{M} + s\mathbf{D} + \mathbf{K})^{-1}\mathbf{P}.$$

In view of the equivalent linearized system (28), the transfer function $\mathbf{H}(s)$ can also be expressed as

$$\mathbf{H}(s) = \mathbf{L}^T(\mathbf{G} + s\mathbf{C})^{-1}\mathbf{B}.$$

The power series expansion of $\mathbf{H}(s)$ about $s = 0$ can be formally written as

$$\mathbf{H}(s) = \mathbf{M}_0 + \mathbf{M}_1s + \mathbf{M}_2s^2 + \dots$$

where \mathbf{M}_i are called (*low-frequency*) *moments*. These moments can be compactly expressed in terms of the linearized system (28) as

$$\mathbf{M}_j = (-1)^j \mathbf{L}^T (\mathbf{G}^{-1} \mathbf{C})^j \mathbf{G}^{-1} \mathbf{B} \quad \text{for } j = 0, 1, 2, \dots,$$

where it is assumed that the matrix \mathbf{K} in (29) is invertible.

3.1. Eigensystem methods

Using the linearization formulation (28) of the second-order system (27), one can immediately use the eigensystem methods of linear systems as discussed in Section 2.1 for the frequency response analysis of the second-order system (27). However, in this section, we exploit the idea of eigensystem methods and treat the second-order system (27) directly.

Assume that the input forced excitation $\mathbf{u}(t)$ of the second-order system (27) is of the harmonic form $\mathbf{u}(t) = \tilde{\mathbf{u}} e^{i\omega t}$ with frequency ω , where $\tilde{\mathbf{u}}$ is a constant vector. Correspondingly, a harmonic form of state variables $\mathbf{q}(t) = \tilde{\mathbf{q}}(\omega) e^{i\omega t}$. When this is substituted into the first equation of (27), it turns out that we need to solve the following parameterized linear system of equations

$$(-\omega^2 \mathbf{M} + i\omega \mathbf{D} + \mathbf{K}) \tilde{\mathbf{q}}(\omega) = \mathbf{P} \tilde{\mathbf{u}} \quad (30)$$

for $\tilde{\mathbf{q}}(\omega)$. This is called the *direct frequency response analysis method* [22,81]. With a given frequency ω_0 , one can use a linear system solver, either direct or iterative, to obtain the desired $\tilde{\mathbf{q}}(\omega_0)$. Recently, efforts have been made to solve such parameterized linear system of equations more efficiently by iterative methods; for examples, see [80,57].

Alternatively, we can try to reduce the cost of solving the large-scale parameterized linear system of Eqs. (30) by first invoking an eigensystem analysis. This is referred as *modal frequency response analysis* in structural dynamics [81]. By transferring coordinates $\tilde{\mathbf{q}}(\omega)$ of the state vector $\mathbf{q}(t)$ to new coordinates $\mathbf{z}(\omega)$,

$$\mathbf{q}(t) \cong \mathbf{W}_k \mathbf{z}(\omega) e^{i\omega t},$$

where \mathbf{W}_k consists of k selected modal shapes to retain the modes whose resonant frequencies lie within the range of forcing frequencies. Then Eq. (30) is approximated by

$$(-\omega^2 \mathbf{M} \mathbf{W}_k + i\omega \mathbf{D} \mathbf{W}_k + \mathbf{K} \mathbf{W}_k) \mathbf{z}(\omega) = \mathbf{P} \tilde{\mathbf{u}}.$$

Multiplying \mathbf{W}_k^T from the left yields a $k \times k$ parameterized linear system of equations with respect to $\mathbf{z}(\omega)$:

$$(-\omega^2 (\mathbf{W}_k^T \mathbf{M} \mathbf{W}_k) + i\omega (\mathbf{W}_k^T \mathbf{D} \mathbf{W}_k) + (\mathbf{W}_k^T \mathbf{K} \mathbf{W}_k)) \mathbf{z}(\omega) = \mathbf{W}_k^T \mathbf{P} \tilde{\mathbf{u}}.$$

The main question now is how to obtain the desired modal shapes \mathbf{W}_k . One can simply extract the desired modal shapes \mathbf{W}_k from eigenvectors of the matrix pair (\mathbf{M}, \mathbf{K}) by ignoring the contribution of the damping term. This is referred to as the *modal superposition method* in the structural dynamics community. It is applicable under the assumption that the damping term is composed of certain structure, for example, the so-called Rayleigh damping $\mathbf{D} = \alpha \mathbf{M} + \beta \mathbf{K}$, where α and β are scalars [22]. In general, one may need to solve the full quadratic eigenvalue problem $(\lambda^2 \mathbf{M} + \lambda \mathbf{D} + \mathbf{K}) \mathbf{w} = 0$ for the desired modal shapes \mathbf{W}_k . In practice, it is often the case that only a relatively small number of modal shapes are necessary, i.e., $k \ll N$. Mathematical theory and numerical techniques for quadratic eigenvalue problems can be found in the recent survey [85] and references therein.

3.2. Reduced-order modeling based on linearization

The reader may notice that the modal superposition method presented in the previous section is a way to construct a reduced-order model for the frequency response analysis. We now discuss how to use the Krylov subspace techniques for the reduced-order modeling of the second-order system (27), without explicitly using modal shapes. One straightforward approach is to apply the Krylov subspace techniques reviewed in Section 2 to the linearized system (28). The approach can be simply outlined as follows:

- (1) Linearize the second-order system (27) by properly defining $2N \times 2N$ matrices \mathbf{C} and \mathbf{G} of the equivalent linear system (28). Select an expansion point s_0 around the frequencies of interest.
- (2) Apply a Krylov process, say the Lanczos process as in Section 2.4, to obtain the left and right projection subspaces $\text{span}\{\mathbf{W}_n\} = \mathcal{K}_n(\mathbf{A}^T, \mathbf{L})$ and $\text{span}\{\mathbf{V}_n\} = \mathcal{K}_n(\mathbf{A}, \mathbf{R})$, where $\mathbf{A} = (\mathbf{G} + s_0\mathbf{C})^{-1}\mathbf{C}$, and $\mathbf{R} = (\mathbf{G} + s_0\mathbf{C})^{-1}\mathbf{B}$.
- (3) Approximate the state vector $\mathbf{x}(t)$ by another state vector $\mathbf{z}(t)$ constrained to the subspace $\text{span}\{\mathbf{V}_n\}$, i.e., let $\mathbf{x}(t) \approx \mathbf{V}_n\mathbf{z}(t)$. This yields the reduced-order model of the second-order system (27) in the following linear formulation:

$$\begin{cases} \mathbf{C}_n \dot{\mathbf{z}}(t) + \mathbf{G}_n \mathbf{z}(t) = \mathbf{B}_n \mathbf{u}(t), \\ \hat{\mathbf{y}}(t) = \mathbf{L}_n^T \mathbf{z}(t), \end{cases}$$

where $\mathbf{C}_n = -\mathbf{T}_n$, $\mathbf{G}_n = (\mathbf{I}_n - s_0\mathbf{D}_n\mathbf{T}_n)$, $\mathbf{R}_n = \mathbf{W}_n^T \mathbf{R}$, and $\mathbf{L}_n = \mathbf{V}_n^T \mathbf{L}$.

In Fig. 10, we demonstrate the numerical results of this approach for a linear-drive multi-mode resonator structure reported in [21]. The solid lines are the Bode plots of frequency responses of the original second-order system of order 63. The dashed lines in the left plot are the Bode plots of frequency responses $H_8(s)$ for the 8th-order linear model and in the right plot are the Bode plots of frequency responses $H_{12}(s)$ of the 12th-order linear model. The relative errors between $H(s)$ and the $H_{12}(s)$ are less than 10^{-4} over the frequency range.

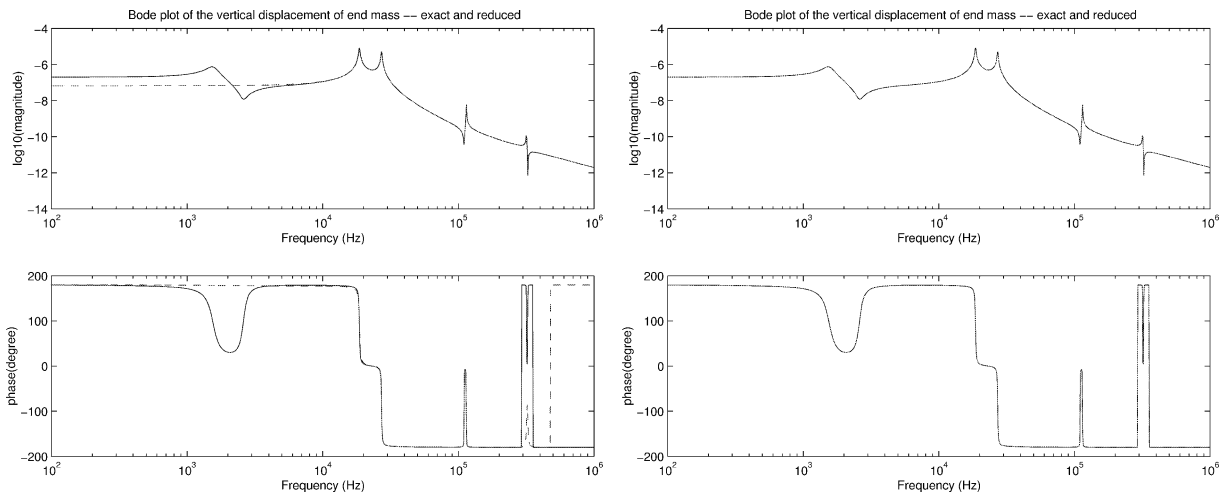


Fig. 10. Bode plots of $H(s)$ and $H_8(s)$ (left) and $H(s)$ and $H_{12}(s)$ (right).

There are a couple of advantages to the linearization approach, namely, one can directly exploit existing reduced-order modeling techniques developed for linear systems, and furthermore, one can also exploit the structures of linearized system matrices C and G in a Krylov process to reduce the computational costs. However, the linearization approach also has a number of disadvantages. Particularly, it ignores the physical meaning of the original system matrices and more importantly, the reduced-order model is no longer in a second-order form. For engineering design and control of dynamical systems, it is highly desirable to have a reduced-order model preserving the second-order form [83].

3.3. Reduced-order modeling based on second-order systems

In this section, we discuss a Krylov subspace method which produces a reduced-order model of the second-order form. This is based on the work of Su and Craig, Jr. [83]. The key observation goes as follows. By the linearization (28) of the second-order system (27), the desired Krylov projection subspace for reduced-order modeling is

$$\mathcal{K}_n(G^{-1}C, \tilde{B}) = \text{span}\{\tilde{B}, (G^{-1}C)\tilde{B}, (G^{-1}C)^2\tilde{B}, \dots, (G^{-1}C)^{n-1}\tilde{B}\}$$

where $\tilde{B} = G^{-1}[B \quad L]$. Let us denote

$$R_j = \begin{bmatrix} R_j^d \\ R_j^v \end{bmatrix} = (G^{-1}C)^j \tilde{B},$$

where R_j^d is an N -vector corresponding to the displacement portion of the vector R_j , and R_j^v is an N -vector corresponding to the velocity portion of the vector R_j , as referred to in [83]. Then by the structure of the matrices C and G , we have

$$\begin{aligned} \begin{bmatrix} R_j^d \\ R_j^v \end{bmatrix} &= (G^{-1}C) \begin{bmatrix} R_{j-1}^d \\ R_{j-1}^v \end{bmatrix} = \begin{bmatrix} K^{-1}D & K^{-1}M \\ -I & 0 \end{bmatrix} \begin{bmatrix} R_{j-1}^d \\ R_{j-1}^v \end{bmatrix} \\ &= \begin{bmatrix} K^{-1}DR_{j-1}^d + K^{-1}MR_{j-1}^v \\ -R_{j-1}^d \end{bmatrix}. \end{aligned}$$

We observe that the j th velocity portion vector R_j^v is the $(j - 1)$ th displacement portion vector R_{j-1}^d (up to the sign difference). In other words, the second portion R_j^v of R_j is a “one-step delay” of the first portion R_{j-1}^d of R_{j-1} . This suggests that one may simply use the first portion of the vectors $\{R_j\}$ and choose

$$\text{span}\{R_0^d, R_1^d, R_2^d, \dots, R_{n-1}^d\}$$

as the projection subspace. In practice, for numerical stability, one may use the Arnoldi process to generate an orthonormal basis Q_n of the desired subspace. The resulting procedure is outlined in Fig. 11. By the *change-of-state coordinates*, namely, approximating the state vector $q(t)$ by another state vector $z(t)$ constrained to the subspace $\text{span}\{Q_n\}$: $q(t) \approx Q_n z(t)$, this immediately yields a reduced-order model of the original system (27) in a second-order form:

$$\begin{cases} M_n \ddot{z}(t) + D_n \dot{z}(t) + K_n z(t) = P_n u(t) \\ \hat{y}(t) = E_n^T z(t), \end{cases} \quad (31)$$

```

(1) Initialization
(2)  $\mathbf{R}_0^d = \mathbf{K}^{-1}[\mathbf{P} \quad \mathbf{E}]$ 
(3)  $\mathbf{R}_0^v = \mathbf{0}$ 
(4)  $(\mathbf{R}_0^d)^T \mathbf{K} \mathbf{R}_0^d = \mathbf{U}_0 \mathbf{S}_0 \mathbf{V}_0^T$  (SVD)
(5)  $\mathbf{Q}_1 = \mathbf{R}_0^d \mathbf{U}_0 \mathbf{S}_0^{-1/2}$ 
(6)  $\mathbf{Q}'_1 = \mathbf{0}$ 
(7) Arnoldi loop
(8) for  $j = 1, 2, \dots, n - 1$  do
(9)    $\mathbf{R}_j^d = \mathbf{K}^{-1}(\mathbf{D} \mathbf{Q}_j + \mathbf{M} \mathbf{Q}'_{j-1})$ 
(10)   $\mathbf{R}_j^v = -\mathbf{Q}_j$ 
(11)  Orthogonalization
(12)  for  $i = 1, 2, \dots, j$  do
(13)     $\mathbf{T}_i = (\mathbf{Q}_i)^T \mathbf{K} \mathbf{R}_j^d$ 
(14)     $\mathbf{R}_j^d = \mathbf{R}_j^d - \mathbf{Q}_i \mathbf{T}_i$ 
(15)     $\mathbf{R}_j^v = \mathbf{R}_j^v - \mathbf{Q}'_i \mathbf{T}_i$ 
(16)  end for
(17)  Normalization
(18)   $(\mathbf{R}_j^d)^T \mathbf{K} \mathbf{R}_j^d = \mathbf{U}_j \mathbf{S}_j \mathbf{V}_j^T$  (SVD)
(19)   $\mathbf{Q}_{j+1} = \mathbf{R}_j^d \mathbf{U}_j \mathbf{S}_j^{-1/2}$ 
(20)   $\mathbf{Q}'_{j+1} = \mathbf{R}_j^v \mathbf{U}_0 \mathbf{S}_0^{-1/2}$ 
(21) end for

```

Fig. 11. Arnoldi process based algorithm for generating basis vectors $\{\mathbf{Q}_j\}$.

where $\mathbf{M}_n = \mathbf{Q}_n^T \mathbf{M} \mathbf{Q}_n$, $\mathbf{D}_n = \mathbf{Q}_n^T \mathbf{D} \mathbf{Q}_n$, $\mathbf{K}_n = \mathbf{Q}_n^T \mathbf{K} \mathbf{Q}_n$, $\mathbf{P}_n = \mathbf{Q}_n^T \mathbf{P}$, and $\mathbf{E}_n = \mathbf{Q}_n^T \mathbf{E}$. In [83], a number of advantages of this approach are credited in terms of preserving stability, symmetry and physical meaning of the original system. Here we present an example for the frequency response analysis of a second-order system of order 400, which comes from a finite element model of a shaft on bearing supports with a damper. The data were extracted from MSC/NASTRAN and are used in [51] to test an algorithm for solving symmetric quadratic eigenvalue problems. In the top of Fig. 12, we plot the magnitudes of the exact transfer function $H(s)$, and approximate ones by the model superposition method (MSP) as discussed in Section 3.1 and by the Krylov subspace method (ROM). For the modal superposition method, we use the 80 mode shapes \mathbf{W}_{80} from the matrix pair (\mathbf{M}, \mathbf{K}) . The reduced-order model (31) is also of order 80. The bottom plot of Fig. 12 shows the relative errors between the exact and approximation based on the modal superposition method (dash-dot line) and the exact and the approximation based on the Krylov subspace method (dashed line). The plots indicate that no accuracy has been lost by the Krylov subspace method. Numerical results are also reported in [71] for simulating the dynamics of a micromirror.

In terms of the moment-matching property, Su and Craig, Jr. [83] show that under the assumption of symmetry of the matrices \mathbf{M} , \mathbf{D} and \mathbf{K} , and the nonsingularity of \mathbf{M} and \mathbf{K} , the reduced-order model (31) matches the first $2n$ moments of the full-order system (27). Precisely, note that the transfer function of the reduced-order model (31) is given by

$$\mathbf{H}_n(s) = \mathbf{E}_n^T (s^2 \mathbf{M}_n + s \mathbf{D}_n + \mathbf{K}_n)^{-1} \mathbf{P}_n$$

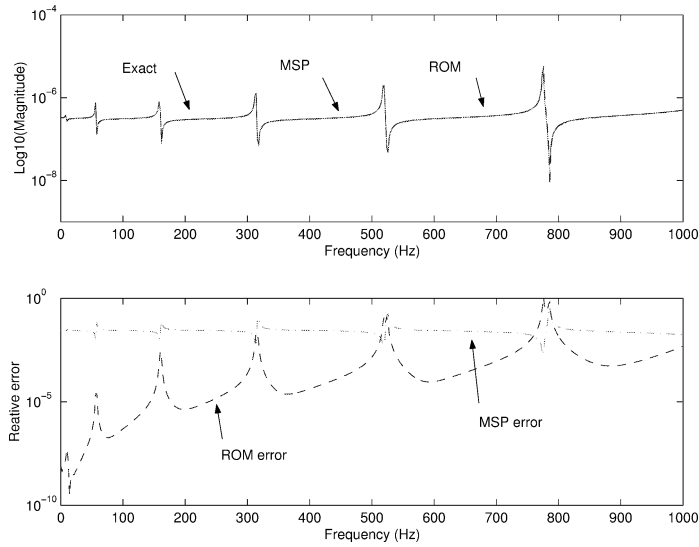


Fig. 12. Comparison of three methods for frequency responses (top) of a shaft on bearing support with a damper (top) and relative errors (bottom).

or equivalently, it can be written in linear form

$$\mathbf{H}_n(s) = \mathbf{L}_n^T (s\mathbf{C}_n + \mathbf{G}_n)^{-1} \mathbf{B}_n,$$

where

$$\mathbf{C}_n = \begin{bmatrix} \mathbf{D}_n & \mathbf{M}_n \\ \mathbf{M}_n & \mathbf{0} \end{bmatrix}, \quad \mathbf{G}_n = \begin{bmatrix} \mathbf{K}_n & \mathbf{0} \\ \mathbf{0} & -\mathbf{M}_n \end{bmatrix}, \quad \mathbf{B}_n = \begin{bmatrix} \mathbf{P}_n \\ \mathbf{0} \end{bmatrix}, \quad \mathbf{L}_n = \begin{bmatrix} \mathbf{E}_n \\ \mathbf{0} \end{bmatrix}.$$

Then the power series expansion of $\mathbf{H}_n(s)$ about $s = 0$ is given by

$$\mathbf{H}_n(s) = \widehat{\mathbf{M}}_0 + \widehat{\mathbf{M}}_1 s + \widehat{\mathbf{M}}_2 s^2 + \dots,$$

where the moments $\widehat{\mathbf{M}}_i$ can be expressed compactly in terms of the corresponding linearized system as

$$\widehat{\mathbf{M}}_j = (-1)^j \mathbf{L}_n^T (\mathbf{G}_n^{-1} \mathbf{C}_n)^j \mathbf{G}_n^{-1} \mathbf{B}_n \quad \text{for } j = 0, 1, 2, \dots$$

Then it can be shown that $\mathbf{H}(s)$ and $\mathbf{H}_n(s)$ match the first $2n$ moments:

$$\mathbf{M}_j = \widehat{\mathbf{M}}_j \quad \text{for } j = 0, 1, 2, \dots, 2n - 1.$$

In other words, $\mathbf{H}(s) = \mathbf{H}_n(s) + \mathcal{O}(s^{2n})$. It is assumed that no deflation occurs in the Krylov process defined in Fig. 11.

There are a number of problems remaining unanswered. For example, can the approach be generalized to the nonsymmetric and possibly singular system matrices \mathbf{M} , \mathbf{D} and \mathbf{K} ? How should we take deflation into account in the Krylov process and what is its effect in terms of the moment-matching property? How do we introduce the shifting strategy to generalize the frequency response analysis around an arbitrary expansion point s_0 ? Work in these directions is in progress and will be reported elsewhere.

4. Semi-second-order dynamical systems

A time-invariant multi-input multi-output second-order system with nonlinear excitation force may be written as a semi-second-order system of the following form:

$$\begin{cases} \mathbf{M}\ddot{\mathbf{q}}(t) + \mathbf{D}\dot{\mathbf{q}}(t) + \mathbf{K}\mathbf{q}(t) = \mathbf{P}\mathbf{u}(\mathbf{q}, \dot{\mathbf{q}}, t), \\ \mathbf{y}(t) = \mathbf{E}^T\mathbf{q}(t), \end{cases} \quad (32)$$

where the system data \mathbf{M} , \mathbf{D} , \mathbf{K} , \mathbf{P} and \mathbf{E} have the same interpretation as in the standard second-order system (27). The exception is that the excitation force \mathbf{u} is not only from external sources, but also could be from internal sources. \mathbf{u} is a nonlinear function of \mathbf{q} and possibly $\dot{\mathbf{q}}$.

Such systems arise in a number of applications, particularly in the emerging area for the simulation of MEMS devices [79]. The semi-second-order system (32) is currently used as the governing equations in SUGAR, a system level simulation package for MEMS devices [84]. For example, Fig. 13 shows a simple electrostatic gap-closing actuator used as a demo in SUGAR, where the excitation force \mathbf{u} includes the electrostatic force between the plates and is proportional to $v(t)^2/\text{gap}(\mathbf{q})^2$, where $v(t)$ is the voltage between electrodes and $\text{gap}(\mathbf{q})$ is a scalar function of \mathbf{q} for the distance between two plate electrodes. For more detail about the description of the electrostatic gap-closing actuator, see [5]. The mathematical model and properties of the electrostatic actuator are also studied in [66].

Instead of treating the semi-second-order system (32) as a general nonlinear system, we can exploit the structure of the system and use the idea of “nonlinear dynamics using linear modes”. This idea is suggested in [1], where a nondamped system ($\mathbf{D} = \mathbf{0}$) is considered and the eigenmodes of \mathbf{M} and \mathbf{K} are used to extract a reduced-order model. In [5], we develop a Krylov subspace based reduced-order modeling technique. We simply first ignore the nonlinearity in the force term \mathbf{u} , and treat the system as an ordinary second-order system. Using the approach as discussed in Section 3.2, a projection subspace \mathbf{V}_n is first constructed, which may be viewed as spanned by *the linear Krylov modes*, and then the state vector \mathbf{q} is expanded in terms of the constructed subspace, namely, $\mathbf{q}(t) \approx \mathbf{V}_n\mathbf{z}(t)$. A reduced-order model in terms of the vector $\mathbf{z}(t)$ is given by

$$\begin{cases} \mathbf{C}_n\dot{\mathbf{z}}(t) + \mathbf{G}_n\mathbf{z}(t) = \mathbf{B}_n\mathbf{u}(\mathbf{V}_n\mathbf{z}(t), t), \\ \tilde{\mathbf{y}}(t) = \mathbf{L}_n^T\mathbf{z}(t), \end{cases}$$

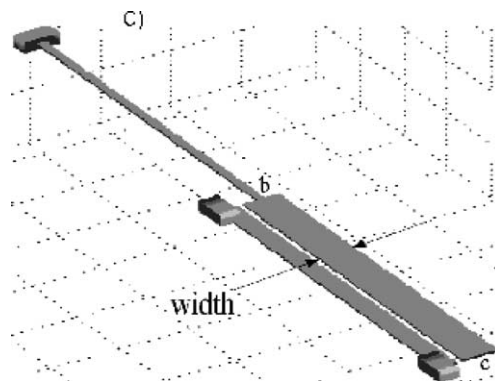


Fig. 13. Electrostatic gap-closing actuator.

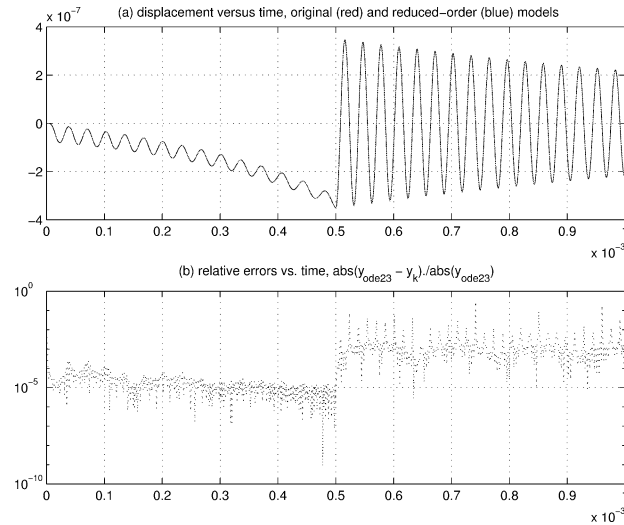


Fig. 14. Transient responses of the gap-closing actuator.

where the definitions of C_n , G_n , B_n and L_n are the same as in Section 3.2. Note that the excitation force term $\mathbf{u}(\mathbf{q}, t)$ of the full-order system is replaced by $\mathbf{u}(\mathbf{V}_n \mathbf{z}, t)$ in the reduced-order model. When the reduced-order model is solved by a numerical method, it is necessary that $\mathbf{u}(\mathbf{V}_n \mathbf{z}_j, t)$ can be efficiently evaluated for a given \mathbf{z}_j , where \mathbf{z}_j is an approximation of $\mathbf{z}(t)$ at time step $t = t_j$.

In Fig. 14, we illustrate this scheme for the transient analysis of the electrostatic actuator shown in Fig. 13. The first plot shows the output $\mathbf{y}(t)$ of the full-order system and the output $\tilde{\mathbf{y}}(t)$ of the reduced-order system. The second plot shows the accuracy of the reduced-order model in terms of the relative error $\|\mathbf{y}(t) - \tilde{\mathbf{y}}(t)\|/\|\mathbf{y}(t)\|$ for the 6th order of the reduced-order model. The order of the original model is $N = 30$. Even for such a small model, we have observed a factor of 60 speedup, see [5] for more details. While a number of satisfactory results are reported based on the idea of “nonlinear dynamics using linear modes”, as indicated in the recent work [36], linear (eigen- or Krylov-)modes may not adequately capture all the features of nonlinear behaviors. It is still the subject of further study to understand this approach and its limitations. We will further discuss this issue in the following section.

5. Nonlinear dynamical systems

Several model reduction techniques for nonlinear dynamical systems have been studied by researchers in various fields. Two of the most well-known methods are the Karhunen–Loève decomposition based methods and methods of balanced truncation. Karhunen–Loève decomposition based methods are also known as proper orthogonal decomposition (POD) methods. Methods of balanced truncation extend the success of balanced truncation of linear systems to nonlinear systems. It is beyond the scope of this paper to review these methods. The interested reader is referred to [46,77]. The latest work includes [52,72]. Means of applying Krylov subspace techniques for adaptively extracting accurate reduced-order models of large-scale nonlinear dynamical systems is a relatively open problem. There has been much current interest in developing such techniques. In this section, we discuss two methods, which extend Krylov subspace techniques for linear dynamical systems as discussed in Section 2.

We consider multi-input multi-output nonlinear dynamical systems of the form:

$$\begin{cases} \dot{\mathbf{x}} = \mathbf{f}(\mathbf{x}) + \mathbf{B}\mathbf{u}, \\ \mathbf{y} = \mathbf{L}^T \mathbf{x} \end{cases} \quad (33)$$

with initial condition $\mathbf{x}(0) = \mathbf{x}_0$, where $\mathbf{x} \in \mathcal{R}^N$ is the state variables, N is the dimension of the state space. $\mathbf{u} \in \mathcal{R}^m$ and $\mathbf{y} \in \mathcal{R}^p$ are inputs and outputs, respectively. $\mathbf{B} \in \mathcal{R}^{N \times m}$ is the input distribution array. $\mathbf{L} \in \mathcal{R}^{N \times p}$ is the output measurement array. We assume that the nonlinear state evolution function $\mathbf{f}(\mathbf{x}) : \mathcal{R}^N \rightarrow \mathcal{R}^N$ is smooth, i.e., C^∞ , and has an equilibrium. Without loss of generality we take this equilibrium at $\mathbf{0}$, i.e., $\mathbf{f}(\mathbf{0}) = \mathbf{0}$.

Examples of the origins of nonlinear dynamical systems of the form (33) include the simulation of time-varying nonlinear circuit elements by independent excitation source [30,19], and MEMS, such as micro-pressure sensor [60]. The modeling of the dynamical behavior of a voltage-controlled parallel-plate electrostatic actuator as shown in Fig. 15 also derives a set of state equations of the form (33) [78, p. 138]. Such an electrostatic actuator invokes multi-domain parameters, such as mass, stiffness and damping in the mechanical domain, and an excitation force network in the electrical domain.

In the following, we discuss two approaches for the reduced-order modeling of the nonlinear system (33). The first approach is called the *linearization method*. It linearizes the system around the equilibrium point, and then extracts a Krylov subspace for reduced-order modeling. Specifically, suppose that the power series expansion of $\mathbf{f}(\mathbf{x})$ about the equilibrium point $\mathbf{0}$ is written

$$\mathbf{f}(\mathbf{x}) = \mathbf{A}_1 \mathbf{x} + \mathbf{A}_2 (\mathbf{x} \otimes \mathbf{x}) + \mathbf{A}_3 (\mathbf{x} \otimes \mathbf{x} \otimes \mathbf{x}) + \dots \quad (34)$$

where $\mathbf{A}_1 \in \mathcal{R}^{N \times N}$ is the Jacobian or the first derivative of \mathbf{f} , and $\mathbf{A}_2 \in \mathcal{R}^{N \times N^2}$ is the second derivative matrix of \mathbf{f} , and so on. \otimes is the Kronecker product. We linearize the original nonlinear system (33) by only using the first term in the expansion (34) of \mathbf{f} , and obtain a linear system:

$$\begin{cases} \dot{\hat{\mathbf{x}}} = \mathbf{A}_1 \hat{\mathbf{x}} + \mathbf{B}\mathbf{u}, \\ \hat{\mathbf{y}} = \mathbf{L}^T \hat{\mathbf{x}}. \end{cases} \quad (35)$$

We can then immediately apply a reduced-order modeling method discussed in Section 2 for the linearized system (35), and obtain a *linear* reduced-order model. The output $\hat{\mathbf{y}}$ is regarded as an approximation of the output \mathbf{y} of the original system (35). If we are interested in a small region of the state space near the equilibrium point, or so-called small-signal analysis, then as demonstrated in [30], this approach provides an efficient tool for analyzing the nonlinear system (33).

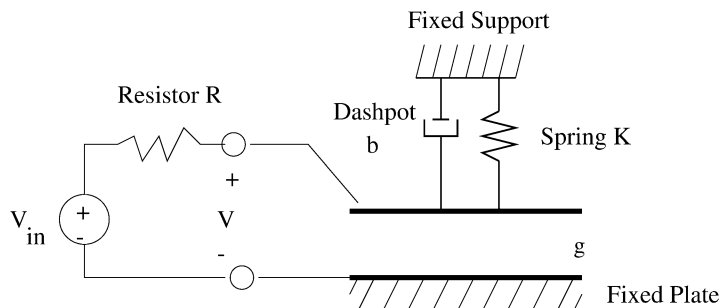


Fig. 15. A voltage-controlled parallel-plate electrostatic actuator includes multi-energy domain parameters [78, p. 138].

Alternatively, one may also use the linearized model (35) to extract a Krylov projection subspace spanned by V_n . Then, by substituting $x \approx V_n z$ into the original nonlinear system (33), a *nonlinear* reduced-order model is obtained:

$$\begin{cases} \dot{z} = g(z) + B_n u, \\ \hat{y} = L_n^T z \end{cases}$$

where $g(z) = V_n^T f(V_n z)$, $B_n = V_n^T B$ and $L_n = V_n^T L$. We assume that V_n is an orthonormal basis of the projection subspace. One of the issues associated with this approach is that one must have a representation of $g(z) = V_n^T f(V_n z)$ that can be efficiently stored and evaluated. The challenge of this issue is highlighted in [60]. If f has a certain structure, then one may exploit such structure to derive an efficient representation of g . For example, in [19,18], f is considered as a quadratic function $f(x) = Ax + J(x \otimes x)$, and in [36], f is represented as a gradient of a scalar function $f(x) = \nabla_x \phi(x)$.

It is often the case that in order to obtain some pre-knowledge about the dynamical behavior of the full-order nonlinear system, we intentionally linearize a system even if it is not near the equilibrium and accept some degree of error rather than confront the full-order nonlinear system. To understand the limitation of this approach, namely, when a reduced-order model strictly based on *linear* information, namely, the Jacobian of the nonlinear state evaluation function f , is accurate enough for a particular application, we may invoke the tool of variational analysis to analyze the contribution of the higher order nonlinear term [74, p. 113]. As a by-product, we may also use the resulting sequence of linearized systems to develop a technique for the reduced-order model of the nonlinear dynamical system. Preliminary results are reported in [68].

The second approach is intended to explicitly incorporate the higher order nonlinear terms in the power series expansion (34) of f into the construction of a Krylov projection subspace. The approach is based on the Carleman bilinearization of a nonlinear system. See, for example, [74,76] for the Carleman bilinearization. The following is an outline of this approach, which is recently suggested in [69]. For simplicity, we consider the single-input single-output case of the nonlinear system (33). By Carleman bilinearization, the nonlinear system (33) can be approximated by a bilinear system given in the following form

$$\begin{cases} \dot{\hat{x}} = \hat{A}\hat{x} + \hat{N}\hat{x}u + \hat{b}u, \\ \hat{y} = \hat{c}^T \hat{x}. \end{cases} \tag{36}$$

Then by applying the multi-dimensional Laplace transform, it can be shown that the k th degree transfer function of the bilinear system (36) is given by

$$H_k(s_1, \dots, s_k) = \hat{c}^T (s_k I - \hat{A})^{-1} \hat{N} \dots \hat{N} (s_2 I - \hat{A})^{-1} \hat{N} (s_1 I - \hat{A})^{-1} \hat{b}. \tag{37}$$

From the power series expansion of $(s_j I - \hat{A})^{-1}$, it is natural to define the corresponding *multi-moments* as

$$m(\ell_1, \ell_2, \dots, \ell_k) = (-1)^n \hat{c}^T \hat{A}^{-\ell_k} \hat{N} \dots \hat{N} \hat{A}^{-\ell_2} \hat{N} \hat{A}^{-\ell_1} \hat{b}, \tag{38}$$

where ℓ_i are nonnegative integers. The expressions of the transfer function (37) and the associated multi-moments (38) suggest that a projection subspace V_n can be constructed by a nest of Krylov subspaces

$$\text{span}\{V_n\} = \mathcal{K}_m(\dots \mathcal{K}_m(\hat{A}^{-1}, \hat{A}^{-1} N \cdot \mathcal{K}_m(\hat{A}^{-1}, \hat{A}^{-1} b)) \dots).$$

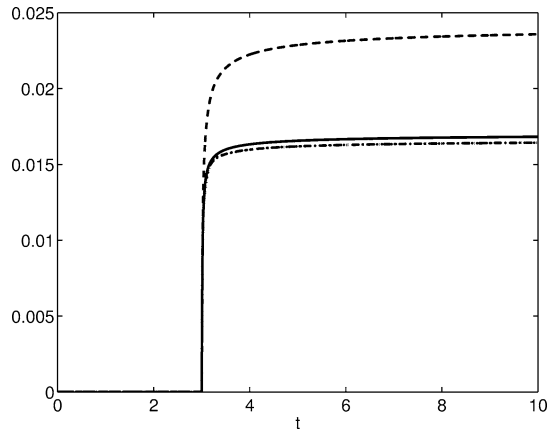


Fig. 16. Transient responses of a nonlinear circuit system, full-order system (solid), reduced-order model of the linearized system (dash), and reduced-order bilinear system (dash-dot).

Once the basis V_n of the projection subspace is extracted, we can approximate the state vector $\hat{x}(t)$ by another state vector $z(t)$ constrained to the subspace $\text{span}\{V_n\}$, i.e., let $\hat{x}(t) \approx V_n z(t)$. This yields a reduced-order modeling of the bilinear system (36):

$$\begin{cases} \dot{z} = \hat{A}_n z + \hat{N}_n z u + \hat{b}_n u, \\ \tilde{y} = \hat{c}_n^T z. \end{cases} \quad (39)$$

This approach can explicitly incorporate higher order nonlinear terms of the state evolution function f and meanwhile an existing Lanczos or Arnoldi process for generating a Krylov projection basis can be applied. However, one critical issue associated with this approach is the rapid growth of the dimension of the bilinear system (36) as a result of Carleman linearization. For example, even if we only use the first two terms in the power series expansion (34) of f , the order of the resulting bilinear system is about $\mathcal{O}(N^2)$. However, the matrices A_i in the power series expansion (34) of f are generally extremely sparse, and the matrices \hat{A} and \hat{N} in the bilinear system (36) are highly structured, so one can exploit these facts in a Krylov process, namely through the matrix–vector multiplications during the Lanczos or Arnoldi process, and produce a useful reduced-order model. In Fig. 16, we show the transient responses of a RC circuit with nonlinear resistors taken from [19]. The dimension of the original full-order nonlinear system is $N = 100$. The solid line is the exact response $y(t)$, computed as the solution of the full-order system. The dashed line is the response of the linearized system (35) of reduced-order 45. The dash-dot line is the response of the bilinear system (39) of the reduced-order 17. The response of the reduced-order bilinear system is significantly more accurate than the linearized system. We have only limited experience with this approach. Work in this direction is still in progress and will be reported in [9].

6. Concluding remarks

An accurate and effective reduced-order model of large-scale dynamical systems can be applied for steady state analysis, modal frequency analysis, transient analysis and sensitivity analysis. As a result, it can significantly reduce design and simulation cycles. Such a computational prototyping tool often speeds

up the process by orders of magnitude. In the past few years, we have witnessed exciting progress in reduced-order modeling of large-scale dynamical systems using Krylov subspace techniques. Numerous efficient algorithms have been developed for the reduced-order modeling of linear and second-order systems. They have demonstrated great success in some applications, such as circuit simulation.

Looking ahead, automatic generation of an accurate and effective reduced-order model directly based on the description of a physical system or device is not only an algorithmic issue, but also a challenging software issue. The development of industrial strength software is necessarily quite involved due to various robustness and efficiency issues related to the underlying Krylov processes. It will be a subject of further study. Reduced-order modeling of large-scale nonlinear dynamical systems is ultimately important and hard. Research into the development of Krylov subspace based techniques has just begun. Meanwhile, new challenges are arising in the simulation of multi-energy domain and multi-scaling systems. Finally, we note that accuracy and integration issues related to the coupling between a reduced-order model of a subsystem and the rest of the system are still open problems.

Acknowledgements

I am grateful to Roland Freund and William Smith for introducing me to the topic, with whom I have had pleasant and productive collaborations. Thanks to Louis Komzsik and Tom Kowalski for providing case studies from structural dynamics. I am also grateful for having the opportunity to work with members of the SUGAR project [84] for developing simulation tools for MEMS, which adds a new dimensional challenge to the research of reduced-order modeling techniques. I would like to thank Daniel Skoogh for producing the plot in Fig. 16. The editors, David Griffiths and Alistair Watson, and the anonymous referee provided valuable suggestions for improvement of the presentation. Support for this work has been provided in part by NSF under grant ACI-9813362 and DOE under grant DE-FG03-94ER25219, and in part by a MICRO project (#00-005) from the University of California and MSC.software Corporation.

References

- [1] G.K. Ananthasuresh, R.K. Gupta, S.D. Senturia, An approach to macromodeling of MEMS for nonlinear dynamic simulation, in: *Microelectromechanical Systems (MEMS)*, in: ASME Dynamics Systems Control (DSC) Ser., Vol. 59, American Society of Mechanical Engineers, New York, 1996, pp. 401–407.
- [2] B.D.O. Anderson, S. Vongpanitlerd, *Network Analysis and Synthesis: A Modern Systems Theory Approach*, Prentice-Hall, Englewood Cliffs, NJ, 1973.
- [3] A.C. Antoulas, D.C. Sorensen, *Approximation of large-scale dynamical systems: An overview*, Technical Report, Electrical and Computer Engineering, Rice University, Houston, TX, February 2001.
- [4] Z. Bai, J. Demmel, J. Dongarra, A. Ruhe, H. van der Vorst (Eds.), *Templates for the Solution of Algebraic Eigenvalue Problems: A Practical Guide*, SIAM, Philadelphia, PA, 2000.
- [5] Z. Bai, D. Bindel, J. Clark, J. Demmel, K.S.J. Pister, N. Zhou, New numerical techniques and tools in SUGAR for 3D MEMS simulation, in: *Technical Proceedings of the Fourth International Conference on Modeling and Simulation of Microsystems*, 2000, pp. 31–34.
- [6] Z. Bai, R. Freund, Eigenvalue-based characterization and test for positive realness of scalar transfer functions, *IEEE Trans. Automatic Control* 45 (2000) 2396–2402.
- [7] Z. Bai, R. Freund, A partial Padé-via-Lanczos method for reduced-order modeling, *Linear Algebra Appl.* 332–334 (2001) 139–164.

- [8] Z. Bai, R. Freund, A symmetric band Lanczos process based on coupled recurrence and some applications, *SIAM J. Sci. Comput.* 23 (2001) 542–562.
- [9] Z. Bai, D. Skoogh, Reduced-order modeling of structured nonlinear systems, work in progress.
- [10] Z. Bai, R.D. Slone, W.T. Smith, Q. Ye, Error bounds for reduced system model by Padé approximation via the Lanczos process, *IEEE Trans. Comput. Aided Design, CAD* 18 (1999) 133–141.
- [11] Z. Bai, Q. Ye, Error estimation of the Padé approximation of transfer functions via the Lanczos process, *Electronic Trans. Numer. Anal.* 7 (1998) 1–17.
- [12] G.A. Baker Jr., P. Graves-Morris, *Padé Approximants*, Cambridge University Press, Cambridge, 1996.
- [13] D.L. Boley, Krylov subspace methods on state-space control models, *Circuit Systems Signal Process* 13 (1994) 733–758.
- [14] S. Boyd, L. El Ghaoui, E. Feron, V. Balakrishnan, *Linear Matrix Inequalities in System and Control Theory*, SIAM, Philadelphia, PA, 1994.
- [15] C. Brezinski, Partial Padé approximation, *J. Approx. Theory* 54 (1988) 210–233.
- [16] O. Brune, Synthesis of a finite two terminal network whose driving-point impedance is a prescribed function of frequency, *J. Math. Phys.* 10 (1931) 191–236.
- [17] A. Bultheel, M. van Barvel, Padé techniques for model reduction in linear system theory: A survey, *J. Comput. Appl. Math.* 14 (1986) 401–438.
- [18] J. Chen, S.M. Kang, An algorithm for automatic model-order reduction of nonlinear MEMS devices, in: *IEEE Inter. Symp. on Circuits and Systems*, Geneva, Switzerland, 2000.
- [19] Y. Chen, J. White, A quadratic method for nonlinear model order reduction, in: *Inter. Conf. on Modeling and Simulation of Microsystems, Semiconductors, Sensors and Actuators*, San Diego, CA, 2000.
- [20] E. Chiprout, M.S. Nakhla, *Asymptotic Waveform Evaluation*, Kluwer Academic, Dordrecht, 1994.
- [21] J.V. Clark, N. Zhou, K.S.J. Pister, MEMS simulation using SUGAR v0.5, in: *Proc. Solid-State Sensors and Actuators Workshop*, Hilton Head Island, SC, 1998, pp. 191–196.
- [22] R.W. Clough, J. Penzien, *Dynamics of Structures*, McGraw-Hill, New York, 1975.
- [23] R.R. Craig Jr, *Structural Dynamics: An Introduction to Computer Methods*, Wiley, New York, 1981.
- [24] R.R. Craig Jr, A.L. Hale, Block-Krylov component synthesis method for structural model reduction, *J. Guid. Control Dyn.* 11 (1988) 562–570.
- [25] C. De Villemagne, R.E. Skelton, Model reductions using a projection formulation, *Int. J. Control* 46 (1987) 2141–2169.
- [26] P. Feldman, R.W. Freund, Efficient linear circuit analysis by Padé approximation via the Lanczos process, *IEEE Trans. Computer Aided Design, CAD* 14 (1995) 639–649.
- [27] R.W. Freund, Reduced-order modeling techniques based on Krylov subspaces and their use in circuit simulation, in: B.N. Datta (Ed.), *Applied and Computational Control, Signals, and Circuits*, Vol. 1, Birkhäuser, Boston, 1999, pp. 435–498.
- [28] R.W. Freund, Band Lanczos method (Section 4.6), in: Z. Bai, J. Demmel, J. Dongarra, A. Ruhe, H. van der Vorst (Eds.), *Templates for the Solution of Algebraic Eigenvalue Problems*, SIAM, Philadelphia, PA, 2000, pp. 80–88.
- [29] R.W. Freund, Krylov-subspace methods for reduced-order modeling in circuit simulation, *J. Comput. Appl. Math.* 123 (2000) 395–421.
- [30] R.W. Freund, P. Feldman, Small-signal circuit analysis and sensitivity computations with the PVL algorithm, *IEEE Trans. Circuits Syst. II* 43 (1996) 577–585.
- [31] R.W. Freund, P. Feldmann, Reduced-order modeling of large linear subcircuits via a block Lanczos algorithm, *Proc. 32nd ACM/IEEE Design Automation Conf.*, ACM, New York, NY, 1995.
- [32] R.W. Freund, P. Feldmann, The SyMPVL algorithm and its applications to interconnect simulation, in: *Proceedings of the 1997 International Conference on Simulation of Semiconductor Processes and Devices*, IEEE, New York, 1997, pp. 113–116.
- [33] R.W. Freund, M.H. Gutknecht, N.M. Nachtigal, An implementation of the look-ahead Lanczos algorithm for non-Hermitian matrices, *SIAM J. Sci. Comput.* 14 (1993) 137–158.
- [34] R.W. Freund, N.M. Nachtigal, An implementation of the QMR method based on coupled two-term recurrences, *SIAM J. Sci. Comput.* 15 (1994) 313–337.
- [35] R.W. Freund, N.M. Nachtigal, QMRPACK: A package of QMR algorithms, *ACM Trans. Math. Software* 22 (1996) 46–77.
- [36] L.D. Gabbay, J.E. Mehner, S.D. Senturia, Computer-aided generation of nonlinear reduced-order dynamic macromodels—I: Non-stress-stiffened case, *J. Microelectromechanical Systems* 9 (2000) 262–269.

- [37] K. Gallivan, E. Grimme, P. Van Dooren, Asymptotic waveform evaluation via a Lanczos method, *Appl. Math. Lett.* 7 (1994) 75–80.
- [38] W. Gao, Y. Zhou, Eigenvalue-based algorithms for testing positive realness of SISO systems, submitted for publication.
- [39] G.H. Golub, J. Kautsky, Calculation of Gauss quadrature with multiple free and fixed knots, *Numer. Math.* 41 (1983) 147–163.
- [40] W.B. Gragg, Matrix interpretations and applications of the continued fraction algorithm, *Rocky Mountain J. Math.* 5 (1974) 213–225.
- [41] W.B. Gragg, A. Lindquist, On the partial realization problem, *Linear Algebra Appl.* 50 (1983) 227–319.
- [42] E. Grimme, Krylov projection methods for model reduction, Ph.D. Thesis, Univ. of Illinois at Urbana-Champaign, 1997.
- [43] E. Grimme, D.C. Sorensen, P. Van Dooren, Model reduction of state space systems via an implicitly restarted Lanczos method, *Numer. Algorithms* 12 (1996) 1–31.
- [44] M.H. Gutknecht, Z. Strakoš, Accuracy of two three-term and three two-term recurrences for Krylov space solvers, *SIAM J. Mat. Anal. Appl.* 22 (2000) 213–229.
- [45] S. Hammarling, Numerical solution of the stable, non-negative definite Lyapunov equation, *IMA J. Numer. Anal.* 2 (1982) 303–323.
- [46] P. Holmes, J.L. Lumley, G. Berkooz, *Turbulence, Coherent Structures, Dynamical Systems and Symmetry*, Cambridge University Press, Cambridge, 1996.
- [47] I.M. Jaimoukha, E.M. Kasenally, Implicitly restarted Krylov subspace methods for stable partial realizations, *SIAM J. Matrix Anal. Appl.* 18 (1997) 633–652.
- [48] I.M. Jaimoukha, E.M. Kasenally, Oblique projection methods for large scale model reduction, *SIAM J. Matrix Anal. Appl.* 16 (1997) 602–627.
- [49] T. Kailath, *Linear Systems*, Prentice-Hall, New York, 1980.
- [50] L. Komzsik, *MSC/NASTRAN, Numerical Methods User's Guide, Version 70.5*, The MacNeal-Schwendler Corporation, Los Angeles, CA, 1998.
- [51] T. Kowalski, Extracting a few eigenpairs of symmetric indefinite matrix pencils, Ph.D. Thesis, University of Kentucky, Lexington, KY, 2000.
- [52] S. Lall, J.E. Marsden, S. Glavaski, A subspace approach to balanced truncation for model reduction of nonlinear control systems, *Int. J. Robust Nonlinear Control*, to appear.
- [53] C. Lanczos, An iteration method for the solution of the eigenvalue problem of linear differential and integral operators, *J. Res. Natl. Bur. Stand* 45 (1950) 225–280.
- [54] A.J. Laub, Efficient calculation of frequency response matrices from state space models, *ACM Trans. Math. Software* 12 (1986) 26–33.
- [55] J.-R. Li, Model reduction of large linear systems via low rank system gramians, Ph.D. Thesis. Massachusetts Institute of Technology, Cambridge, MA, 2000.
- [56] R. Li, Test positive realness of a general transfer function, Technical Report 2000-20, Department of Mathematics, University of Kentucky, Lexington, KY, 2000.
- [57] K. Meerbergen, The solution of parameterized linear systems arising from engineering applications. Part I: linear parameter, Technical Report KM-2000-2, Free Field Technologies, Louvain-la-Neuve, Belgium, 2000, submitted for publication.
- [58] G. Meurant, A review of the inverse of symmetric tridiagonal and block tridiagonal matrices, *SIAM J. Mat. Anal. Appl.* 13 (1992) 707–728.
- [59] B.C. Moore, Principal component analysis in linear systems: controllability, observability, and model reduction, *IEEE Trans. Automat. Contr.* 26 (1981) 17–32.
- [60] T. Mukherjee, G. Fedder, D. Ramaswamy, J. White, Emerging simulation approaches for micromachined devices, *IEEE Trans. CAD* 19 (2000) 1572–1588.
- [61] B. Nour-Omid, R.W. Clough, Dynamics analysis of structures using Lanczos coordinators, *Earthquake Eng. Struct. Dyn.* 12 (1984) 565–577.
- [62] A. Odabasioglu, M. Celik, L.T. Pileggi, Practical considerations for passive reduction of RLC circuits, in: *Proc. Inter. Conf. Computer Aided Design*, 1999, pp. 214–219.
- [63] A. Odabasioglu, M. Celik, L.T. Pileggi, PRIMA: Passive reduced-order interconnect macromodeling algorithm, in: *Tech. Dig. 1997 IEEE/ACM International Conference on Computer-Aided Design*, IEEE, New York, 1997, pp. 58–65.
- [64] B. Parlett, Reduction to tridiagonal form and minimal realizations, *SIAM J. Mat. Anal. Appl.* 13 (2) (1992) 567–593.

- [65] B. Parlett, I. Dhillon, Relatively robust representation of symmetric tridiagonal, *Linear Algebra Appl.* 309 (2000) 121–151.
- [66] J.A. Pelesko, Multiple solutions in electrostatic MEMS, in: *Technical Proceedings of the Fourth International Conference on Modeling and Simulation of Microsystems*, 2000, pp. 290–293.
- [67] T. Penzl, A cyclic low-rank Smith method for large sparse Lyapunov equations, *SIAM J. Sci. Comput.* 21 (2000) 1401–1418.
- [68] J. Phillips, Automated extraction of nonlinear circuit macromodels, in: *Proceedings of IEEE 2000 Custom Integrated Circuits Conference*, 2000, pp. 451–452.
- [69] J. Phillips, Projection frameworks for model reduction of weakly nonlinear systems, in: *Proceedings of DAC 2000*, 2000, pp. 184–189.
- [70] L.T. Pillage, R.A. Rohrer, Asymptotic waveform evaluation for timing analysis, *IEEE Trans. Comput. Aided Design* 9 (1990) 353–366.
- [71] D. Ramaswamy, J. White, Automatic generation of small-signal dynamic macromodels from 3-D simulation, in: *Technical Proceedings of the Fourth International Conference on Modeling and Simulation of Microsystems*, 2000, pp. 27–30.
- [72] M. Rathinam, L. Petzold, An iterative method for simulation of large scale modular systems using reduced order models, in: *Proc. IEEE Control and Decision Conference*, Australia, 2000.
- [73] A.E. Ruehli, Equivalent circuit models for three-dimensional multiconductor systems, *IEEE Trans. Microwave Theory Tech.* 22 (1974) 216–221.
- [74] W.J. Rugh, *Nonlinear System Theory*, The John Hopkins University Press, Baltimore, MA, 1981.
- [75] A. Ruhe, Implementation aspects of band Lanczos algorithms for computation of eigenvalues of large sparse symmetric matrices, *Math. Comp.* 33 (1979) 680–687.
- [76] S. Sastry, *Nonlinear Systems: Analysis, Stability and Control*, Springer, New York, 1999.
- [77] J.M.A. Scherpen, Balancing for nonlinear systems, *Systems and Control Letters* 21 (1993) 143–153.
- [78] S.D. Senturia, *Microsystem Design*, Kluwer Academic, Boston, 2001.
- [79] S.D. Senturia, N. Aluru, J. White, Simulating the behavior of MEMS devices: Computational methods and needs, *IEEE Comput. Sci. Engrg.* 4 (1997) 30–43.
- [80] V. Simoncini, Linear system with a quadratic parameter and application to structural dynamics, in: D.R. Kincaid, A.C. Elster (Eds.), *Iterative Methods in Scientific Computation II*, IMACS, 1999, pp. 1–11.
- [81] G. Sittton, *MSC/NASTRAN Basic Dynamic Analysis User's Guide*, The MacNeal-Schwendler Corporation, Los Angeles, CA, 1997.
- [82] D.C. Sorensen, A.C. Antoulas, Projection methods for balanced model reduction, Technical Report, Electrical and Computer Engineering, Rice University, Houston, TX, March 2001.
- [83] T.-J. Su, R.R. Craig Jr., Model reduction and control of flexible structures using Krylov vectors, *J. Guid. Control Dyn.* 14 (1991) 260–267.
- [84] SUGAR, A MEMS simulation program, ver.2.0(beta), August, 2001. Available at <http://www-bsac.eecs.berkeley.edu/~cfm>.
- [85] F. Tisseur, K. Meerbergen, The quadratic eigenvalue problem, *SIAM Rev.* 43 (2001) 235–286.
- [86] P. Van Dooren, Gramian based model reduction of large-scale dynamical systems, in: D.F. Griffiths, G.A. Watson (Eds.), *Numerical Analysis 1999*, Chapman and Hall, London, 2000, pp. 231–247.
- [87] J. Vlach, K. Singhal, *Computer Methods for Circuit Analysis and Design*, Van Nostrand Reinhold, New York, 1994.
- [88] K. Willcox, J. Peraire, J. White, An Arnoldi approach for generalization of reduced-order models for turbomachinery, FDRL TR-99-1, Fluid Dynamic Research Lab., Massachusetts Institute of Technology, 1999, *Comput. Fluids*, submitted.
- [89] Q. Ye, A convergence analysis for nonsymmetric Lanczos algorithms, *Math. Comp.* 56 (1991) 677–691.